11-15-1994

Orbital Studies of the Cataclysmic Variables CZ Orionis, V1193 Orionis and BZ Ursae Majoris

F. A. Ringwald
Dartmouth College

J. R. Thorstensen
Dartmouth College

R. M. Hamwey
Dartmouth College

Mon. Not. R. Astron. Soc. **271**, 323–342 (1994)

Orbital studies of the cataclysmic variables CZ Orionis, V1193 Orionis and BZ Ursae Majoris

F. A. Ringwald,[1,2]★ John R. Thorstensen[2] and R. M. Hamwey[2]

[1] *Department of Physics, Keele University, Keele, Staffordshire ST5 5BG*

[2] *Department of Physics and Astronomy, Dartmouth College, Hanover, New Hampshire, 03755-3528, USA*

Accepted 1994 June 15. Received 1994 June 10; in original form 1993 June 20

ABSTRACT

Time-resolved spectroscopy reveals the orbital periods of three cataclysmic variables. CZ Ori has an orbital period of 0.2189 d. This is within 3 per cent of a prediction relating orbital period and dwarf nova outburst decline time. We find the M2.5 ± 1.0 secondary, and infer an absolute magnitude for CZ Ori in R_{KC} of 8.5 ± 1.0 and a distance of 260 ± 110 pc.

V1193 Ori, also called Hamuy's Blue Variable, has an orbital period of 0.165 d. In 1988, Hα emission line profile variations suggested red star illumination. In 1989, this line's red wing flared at orbital phases 0.2 and 0.8. We set limits for the absolute magnitude in R_{KC} of < 5.9 and for the distance of > 470 pc.

BZ UMa has an orbital period of 0.0679 d, shown by Hα radial velocities and an *S*-wave. The velocities have anomalous low-frequency variations, strongest in the line wings. This rumbling, observed during all three observing runs, is of amplitude comparable to the orbit's. Explanations of instrumental effects, magnetism or disc waves are considered. The M5.5 ± 0.5 secondary implies an absolute magnitude for BZ UMa in R_{KC} of 10.7 (+0.7/−0.9) and a distance of 110 (+44/−51) pc.

Key words: binaries: spectroscopic – stars: fundamental parameters – stars: individual: BZ UMa – stars: individual: CZ Ori – stars: individual: V1193 Ori – novae, cataclysmic variables.

1 INTRODUCTION

The orbital period (P_{orb}) of a cataclysmic variable binary star (CV) is among the few parameters it has that is both directly measurable and not model-dependent. Without it, one knows little about a CV, since the period influences its secular evolution, luminosity and outbursts (Shafter, Wheeler & Cannizzo 1986). The catalogues of Patterson (1984), Webbink (1992, unpublished) and Ritter & Kolb (1994) include only CVs of known or suspected period, emphasizing this parameter's importance. Recent CV reviews include those by Livio (1994) and La Dous (1993).

Radial velocity studies determine periods more reliably than do photometric modulations, save for eclipses, but are not without problems. Orbital semi-amplitudes, or *K*-velocities, are notoriously hard to determine reliably. The emission lines one measures form in the accretion disc, which is not necessarily centred on the white dwarf's centre of mass: $K_{em} \neq K_{WD}$. Since K_{em} is found by fitting sinusoids to the measured velocities, the same problem applies to γ_{em}, the emission line mean velocity, and to T_0, the epoch of spectroscopic phase zero. Eclipsing systems sometimes show T_0 lagging the eclipse by over 70° in phase (e.g. Thorstensen et al. 1991).

This paper reports radial velocity studies of three CVs, namely, CZ Orionis, V1193 Orionis and BZ Ursae Majoris. Tables 1(a)–(c) present the derived orbital parameters for all. Figs 1, 4 and 9–11 show the CVs' spectra, with descriptions for each in Tables 2(a) and (b). In Section 2, observational procedure, data reduction and analysis are described. The individual CVs are discussed in Sections 3–5, and we conclude in Section 6.

2 OBSERVATIONS

The instrumental setups and journals of observations are shown in Tables 3, 4(a) and (b). For all observations, we used Michigan–Dartmouth–MIT Observatory's 1.3-m McGraw–Hill telescope, both Mark III all-transmission Cassegrain spectrographs and either a Thomson or a TI-4849 CCD

★ Internet: far@astro.keele.ac.uk.

Table 1. (a) CZ Ori – derived orbital parameters.[a]

Object	P_{orb} (days)	K_{em} (km s^{-1})	γ_{em} (km s^{-1})	T_0 (HJD − 2440000)	σ (km s^{-1})
1988 January[b]	0.2189 ± 0.0002	61 ± 3	−8 ± 2	7170.073 ± 0.002	13
Before Outburst					
Core[c]	(0.2189)	58 ± 5	2 ± 3	7170.067 ± 0.003	12
Wings[d]	(0.2189)	63 ± 6	−7 ± 4	7170.075 ± 0.003	14
Outburst Decline					
Core[c]	(0.2189)	37 ± 4	−6 ± 3	7170.066 ± 0.003	9
Wings[d]	(0.2189)	54 ± 7	−23 ± 5	7170.078 ± 0.003	16
Alias 2[b]	0.1799 ± 0.0005	57 ± 11	−17 ± 9	7170.032 ± 0.006	15

[a]Velocities fitted to $V(t) = \gamma_{em} + K_{em} \sin[2\pi(t - T_0)/P_{orb}]$; all errors are to 68 per cent confidence (see Thorstensen & Freed 1985).
[b]Measured with the double-Gaussian algorithm, Gaussian separation 750 km s^{-1}.
[c]Measured with the Schneider–Young algorithm, FWHM 300 km s^{-1}.
[d]Measured with the double-Gaussian algorithm, Gaussian separation 970 km s^{-1}.

Table 1. (b) V1193 Ori – derived orbital parameters.[a]

Object	P_{orb} (days)	K_{em} (km s^{-1})	γ_{em} (km s^{-1})	T_0 (HJD − 2440000)	σ (km s^{-1})
1988 January[b]	0.1654 ± 0.0002	95 ± 7	61 ± 5	7169.959 ± 0.002	27
Co-added	(0.165)	91 ± 4	61 ± 3	7169.961 ± 0.001	10
1989 November[c]	0.1653 ± 0.0009	51 ± 6	94 ± 4	7843.750 ± 0.003	21
Co-added	(0.165)	47 ± 10	95 ± 7	7843.749 ± 0.005	22
Core					
1988 January[d]	0.1655 ± 0.0002	97 ± 6	58 ± 5	7169.957 ± 0.002	26
Co-added	(0.165)	93 ± 4	59 ± 3	7169.961 ± 0.001	10
1989 November	0.1648 ± 0.0005	60 ± 5	79 ± 3	7843.754 ± 0.002	17
Co-added	(0.165)	54 ± 7	84 ± 5	7843.753 ± 0.003	15

[a]Velocities fitted to $V(t) = \gamma_{em} + K_{em} \sin[2\pi(t - T_0)/P_{orb}]$; all errors are to 68 per cent confidence (see Thorstensen & Freed 1985).
[b]Measured with the double-Gaussian algorithm, Gaussian separation 540 km s^{-1}.
[c]Measured with the double-Gaussian algorithm, Gaussian separation 690 km s^{-1}.
[d]Measured with Schneider–Young algorithm, Gaussian separation 690 km s^{-1}.

Table 1. (c) BZ UMa – derived orbital parameters.[a]

Object	P_{orb} (days)	K_{em} (km s^{-1})	γ_{em} (km s^{-1})	T_0 (HJD − 2440000)	σ (km s^{-1})
1988 Raw Orbit[b]	0.0679 ± 0.0001	30 ± 11	21 ± 7	7169.987 ± 0.004	32
QPV[c]	0.292 ± 0.001	36 ± 7	−12 ± 5	7170.035 ± 0.009	21
Orbit Only	0.06791 ± 0.00009	31 ± 7	21 ± 5	7169.989 ± 0.002	20
1989 Raw Orbit[b]	0.0679 ± 0.0001	36 ± 6	22 ± 4	7603.960 ± 0.002	39
QPV 1[c]	0.743 ± 0.004	42 ± 4	3 ± 3	7604.11 ± 0.01	17
QPV 2	1.60 ± 0.02	27 ± 4	1 ± 2	7603.33 ± 0.03	17
[QPV 3	0.1306 ± 0.0005	9 ± 3	0 ± 2	7603.945 ± 0.007	17]
Orbit Only	0.06793 ± 0.00004	36 ± 3	22 ± 2	7603.8247 ± 0.0008	17
1991 Raw Orbit[b]	0.0680 ± 0.0002	42 ± 14	1 ± 10	8319.899 ± 0.004	44
QPV	0.1271 ± 0.0004	36 ± 11	−3 ± 8	8319.849 ± 0.006	36
Orbit Only	0.0679 ± 0.0001	39 ± 11	1 ± 8	8319.897 ± 0.003	35

[a]Velocities fitted to $V(t) = \gamma_{em} + K_{em} \sin[2\pi(t - T_0)/P_{orb}]$; all errors are to 68 per cent confidence (see Thorstensen & Freed 1985).
[b]Measured for individual variations with the double-Gaussian algorithm, separation 1370 km s^{-1}.
[c]QPV ≡ Quasi-periodic variation: velocity variation, not strictly periodic (note changes between epochs), which fits a sinusoid and is not a time series sampling artefact (see text).

(Luppino 1989), both of which were geometrically similar. In 1988, we used a 600 line mm^{-1} grism, blazed at λ5800 Å, delivering 5.5-Å resolution at 2.5 Å $channel^{-1}$. All other observations used a 300 line mm^{-1} grism, blazed at λ6400 Å, obtaining 11-Å resolution at 5.0 Å $channel^{-1}$.

Since CVs have such blue colours, a Hoya Y-50 order-blocking filter was used with the reddest setups, in 1989 November and 1991 June. Spectra of hot stars were taken during these runs, to map and remove the telluric absorption bands (see Wade & Horne 1988). Flux standards (Oke 1974) were observed, to remove the instrumental response. The narrow (2.2 arcsec) slit precluded absolute spectrophotometry to within 30 per cent, but did allow accurate digital sky subtraction. Instrumental rotation was deemed unnecessary for such red setups.

Wavelength scales were calibrated with Ar, Hg–Ne, Ne and Xe lamps at the beginning of each night. While observing, we took Ne spectra, nominally every 20–30 min, to monitor shifts in the wavelength scale from spectrograph flexure. Slit-viewing TV autoguiding on guide stars minimized velocity drifts.

All CCD frames were debiased and flat-fielded with the median of nine or more exposures of a tungsten lamp inside the spectrograph, taken each run. Those taken with the TI-4849 were also dark-subtracted, with the median of nine or more dark frames taken each run of the same exposure time as the target frames, typically 15 min. All times were written as heliocentric Julian dates of mid-integration, and all velocities were heliocentrically corrected. The rms residuals of fifth-order polynomial fits set wavelength scales accurate to within 0.10 Å and reproducible to within 0.05 Å for all spectra. Object columns were simply summed together to increase the signal-to-noise ratio (S/N), and cosmic-ray hits were interpolated over. All flux-calibrated spectra were corrected for atmospheric extinction.

Velocities were measured from the Hα emission line in two ways. The first algorithm, that of Schneider & Young (1980), measured the motion of the line core by convolving the line with the derivative of a Gaussian of specified width (FWHM), and taking the zero of this convolution as the velocity. The second algorithm, also of Schneider & Young (1980) and used by Shafter (1983), measured the motion of the line wings by convolving the line with a positive and a negative Gaussian of specified width and separation, and taking the zero of this convolution as the velocity. This allowed the line core and presumably any ill-understood low-velocity motions in it (such as disc turbulence) to be ignored. Whenever using the double-Gaussian method, we used a Gaussian width of 2.8 channels, or 640 km s^{-1}, which at just over one resolution element was wide enough to average out spurious velocity shifts from noise variations. Also whenever using the double-Gaussian method, we varied the separation of the Gaussians to maximize the figure of merit, K_{em}/σ. Formal errors for the ensemble, quoted in

Table 2. (a) Emission lines in summed spectra.

	Hβ 4861	He I 5876	Hα 6563	He I 6678	He I 7065
CZ Ori					
1988 January					
W(Å)	–	–	22	3	3
FWHM (km s^{-1})	–	–	510	890	2200:
FWZI (km s^{-1})	–	–	2600	1600	2400
I/I_{cont}	–	–	2.5	1.2	1.1
1989 November					
W(Å)	39	11	42	4	5:
FWHM (km s^{-1})	950	1100	800	950	1600
FWZI (km s^{-1})	3200	2200	3000	1700	3000:
I/I_{cont}	3.2	1.5	3.4	1.2	1.1
V1193 Ori					
1988 January					
W(Å)	–	–	23	1.5	0.7
FWHM (km s^{-1})	–	–	640	540	410
FWZI (km s^{-1})	–	–	4100	1200	1500:
I/I_{cont}	–	1.1:	2.3	1.1	1.1
1989 November					
W(Å)	4.0	2.4	19	1.2	1.2
FWHM (km s^{-1})	780	570	780	680	650
FWZI (km s^{-1})	1600	1100	3400	1600	1500
I/I_{cont}	1.3	1.2	2.0	1.1	1.1
BZ UMa					
1988 January					
W(Å)	–	79	285	43	50:
FWHM (km s^{-1})	–	1580	1290	1340	1800:
FWZI (km s^{-1})	–	2500	4000	3800	2400
I/I_{cont}	–	3.0	11.3	2.1	2.6:

Table 2. (b) Emission lines in summed spectra.

	Hγ 4340	He I 4471	He II 4686	Hβ 4861	He I 4921	He I (5015)	Fe II 5169	He I 5876	Hα 6563	He I 6678
BZ UMa – 1989 March										
W(Å)	71	29	13	118	14	28	–	69	198	29
FWHM (km s^{-1})	1790	1960	3570	1600	1690	blend	blend	1550	1340	1550
FWZI (km s^{-1})	4900	3600	5200	4100	2800	blend	blend	4200	3800	2900
I/I_{cont}	4.2	2.1	1.3	6.0	1.5	1.6	1.4	3.0	7.2	1.8

	Hα 6563	He I 6678	He I 7065	He I 7281	O I 7773	8200 bump	Pa18 8438	Ca II blend	Pa14 8598	Ca II 8662	Pa12 8750	Pa11 8862
1991 June												
W(Å)	235	34	28	7.2	6.0	5:	1.3	33	2.2	32	15	21
FWHM	1250	1550	1650	1970	1650	3000	1250	blend	1100	1450	1680	1540
FWZI	4050	4100	3700	3100	1650	3870	1750	blend	1600	2800	2760	2730
I/I_{cont}	9.2	2.0	1.7	1.2	1.15	1.09	1.08	1.6	1.8	1.8	1.3	1.6

Table 3. Instrumental setups.

Epoch	CCD	Observer	Range (Å)	$\Delta\lambda$ (Å)
1988 January	Thomson	RMH	5900–7100	5.5
1989 March	Thomson	FAR	4200–6750	11.0
1989 November	TI-4849	JRT	5500–8300	11.0
1991 June	TI-4849	FAR	6200–8940	11.0

Table 4. (a) Hα emission radial velocities: CZ Ori and V1193 Ori.[a]

MHJD[b]	V (km s^{-1})	MHJD[b]	V (km s^{-1})	MHJD[b]	V (km s^{-1})	MHJD[b]	V (km s^{-1})
CZ Ori (1988 January)[c]							
7167.735	70	7167.867	−32	7170.904	−73	7172.854	−60
7167.749	53	7167.883	9	7170.918	−51	7172.861	−62
7167.765	1	7167.898	18	7171.882	77	7172.869	−60
7167.779	−22	7167.913	26	7172.791	18	7172.880	−73
7167.794	−34	7167.928	46	7172.806	−12	7172.894	−58
7167.808	−46	7169.899	37	7172.821	−34	7172.909	−32
7167.824	−70	7169.920	19	7172.835	−44	7172.924	6
7167.838	−71	7170.874	−61	7172.849	−72		
V1193 Ori (1988 January)[d]							
7169.679	137	7169.802	91	7170.830	155	7172.696	−11
7169.690	114	7169.813	109	7170.847	122	7172.707	−58
7169.702	60	7169.824	129	7171.787	54	7172.719	−45
7169.712	74	7169.841	120	7171.798	113	7172.729	−30
7169.724	5	7170.775	19	7171.809	142	7172.741	−28
7169.735	22	7170.786	80	7171.820	197	7172.752	−15
7169.752	−11	7170.797	151	7171.831	181	7172.763	14
7169.774	13	7170.808	149	7171.842	163	7172.774	45
7169.791	50	7170.819	145	7172.679	105		
V1193 Ori (1989 November)[d]							
7842.744	64	7843.039	6	7843.800	168	7843.980	122
7842.751	47	7843.735	62	7843.809	155	7843.990	97
7842.759	43	7843.742	52	7843.817	117	7843.997	93
7842.767	88	7843.750	55	7843.824	104	7844.004	74
7842.775	77	7843.761	76	7843.833	58	7844.013	63
7842.782	117	7843.769	102	7843.840	77	7844.020	30
7843.017	81	7843.776	127	7843.848	56	7844.028	46
7843.025	30	7843.786	136	7843.966	143	7844.035	37
7843.032	38	7843.793	161	7843.973	96		

[a]Velocities fitted to $V(t)=\gamma_{em}+K_{em}\sin[2\pi(t-T_0)/P_{orb}]$; all errors are to 68 per cent confidence (see Thorstensen & Freed 1985).
[b]Heliocentric Julian Date of mid-integration, minus 2 440 000.
[c]Double-Gaussian algorithm, Gaussian separation 750 km s^{-1}.
[d]Schneider–Young (1980) algorithm, 690 km s^{-1} FWHM.

Table 4. (b) Hα emission radial velocities: BZ UMa.[a]

MHJD[b]	V (km s^{-1})	MHJD[b]	V (km s^{-1})	MHJD[b]	V (km s^{-1})	MHJD[b]	V (km s^{-1})
BZ UMa (1988 January)[c]							
7167.974	16	7169.012	−17	7170.972	48	7173.001	63
7167.995	−15	7169.027	−44	7170.995	14	7173.012	41
7168.017	17	7169.951	−52	7171.018	73	7173.023	11
7168.951	20	7169.974	−27	7171.038	91	7173.035	4
7168.969	24	7169.996	6	7172.966	−21	7173.045	53
7168.983	47	7170.018	17	7172.976	41		
7168.998	20	7170.950	22	7172.989	76		
BZ UMa (1989 March)[c]							
7600.751	11	7601.794	42	7603.685	37	7605.784	8
7600.762	15	7601.807	74	7603.696	67	7605.795	56
7600.775	31	7601.819	23	7603.708	69	7605.807	111
7600.788	76	7601.831	−11	7603.720	72	7605.819	77
7600.800	34	7601.842	−22	7603.731	31	7605.831	40
7600.812	−6	7601.854	43	7603.743	24	7605.842	16
7600.822	30	7601.866	81	7604.661	10	7605.854	23
7600.832	−5	7601.878	96	7604.677	−79	7605.866	51
7600.845	24	7601.890	58	7604.690	−100	7605.877	54
7600.858	45	7601.901	26	7604.702	−79	7605.889	42
7600.870	−6	7601.913	54	7604.713	−11	7605.901	5
7600.883	−29	7601.925	79	7604.725	−27	7605.908	54
7600.895	−23	7602.630	67	7604.737	−20	7605.915	−22
7600.907	−12	7602.642	15	7604.749	−70	7605.928	19
7600.919	25	7602.654	17	7605.634	40	7607.662	−41
7600.932	0	7602.666	43	7605.645	36	7607.674	−61
7601.683	−30	7602.678	87	7605.658	63	7607.686	−65
7601.695	−66	7602.690	69	7605.670	77	7607.698	−38
7601.708	−64	7602.702	40	7605.682	107	7607.709	24
7601.720	−20	7602.714	−2	7605.696	62	7607.721	11
7601.732	30	7602.726	−33	7605.724	48	7607.733	−6
7601.746	41	7602.738	26	7605.736	78	7607.745	−49
7601.758	−21	7603.649	86	7605.747	87		
7601.770	−40	7603.661	36	7605.760	40		
7601.782	0	7603.673	29	7605.772	14		
BZ UMa (1991 June)[c]							
8318.863	−85	8318.941	−75	8319.807	−35	8319.885	−15
8318.874	50	8318.952	−30	8319.819	−25	8319.896	23
8318.886	84	8318.963	4	8319.830	2	8323.899	−35
8318.896	19	8318.980	105	8319.841	38	8323.909	3
8318.908	−59	8319.774	30	8319.852	49	8323.923	46
8318.918	−85	8319.785	44	8319.863	27	8323.933	33
8318.930	−114	8319.796	13	8319.874	7	8323.945	13

[a]Velocities fitted to $V(t)=\gamma_{em}+K_{em}\sin[2\pi(t-T_0)/P_{orb}]$; all errors are to 68 per cent confidence (see Thorstensen & Freed 1985).
[b]Heliocentric Julian Date of mid-integration, minus 2 440 000.
[c]Double-Gaussian algorithm, Gaussian separation 1370 km s^{-1}.

Tables 1(a)–(c), were calculated with the likelihood ratio test of Cash (1979). Errors of the individual velocities were about 10 km s^{-1}, estimated by Monte Carlo simulations and measurement of night-sky lines [see Section 5.4(i)].

Lomb–Scargle periodograms (Press et al. 1992) were calculated for a range of frequencies corresponding to periods from 51 min to 10 d, spanning the entire expected range of orbital periods (Ritter & Kolb 1994). These periodograms would have shown periodicities in the unevenly sampled velocities as peaks, much as Fourier spectra do for evenly sampled data. Aliasing, due to interruptions in data acquisition (daylight, clouds etc.), could have caused fringing and created spuriously significant periodogram peaks, but, with the Monte Carlo analysis of Thorstensen & Freed (1985), we estimated the correctness likelihood of choosing the correct alias and the discriminatory power of the time series to make the proper choice. This analysis tested the quality of the time series, not the velocity measurements, but this was crucial: the highest quality spectra would have been useless for finding P_{orb} if sampled in time poorly.

In another test, we generated an artificial sinusoid with the orbital period and other parameters (namely T_0, K_{em} and γ_{em}, as defined in Table 1a) derived from a least-squares fit to the measured velocities. We gave this artificial sinusoid enough random noise to set σ, its standard deviation from a true sinusoid, to 10–15 per cent more than the σ of the data, since, without noise, period determination would be trivial.

Sampling the artificial sinusoid at the observation times, we measured velocities and generated a periodogram. If this 'fake' periodogram looked like the real one, derived from the observations, it increased confidence that the form of the real periodogram resulted only from the sampling. This test proved interesting in the analyses of all three CVs, as we shall see.

3 CZ ORIONIS

CZ Ori, the longest-known and most-observed CV discussed here, was discovered by Hoffmeister (1928) and has been monitored by the AAVSO, BAA and VSS, RASNZ ever since. Szkody & Mattei (1984) analysed its long-term light curve and classified it as a U Gem star, with normal outbursts only. On average, CZ Ori ranges from $V=15.5$ in quiescence to $V=12.1$ in outburst. Although its outburst durations can be short, long and anomalously long (2–12 and 16 d), bimodality is unclear. Williams (1983) and Bruch, Fischer & Wilmsen (1987) gave coordinates and finding charts; Williams (1983) and Szkody (1987) presented blue spectra.

3.1 Spectrum, red star and orbit

We obtained time-resolved spectra for CZ Ori in 1988 January and in 1989 November. The spectrum typified that of a dwarf nova, with the characteristic strong, broad Hα line and weak He I lines all in emission (see Fig. 1 and Tables 1a and 2a). The O I λ7773-Å triplet, probably a disc feature, was broad (FWHM of 790 km s^{-1}, FWZI of 1310 km s^{-1}) and weakly in emission ($I/I_{\rm cont}$ of 1.1, equivalent width of 1.6 Å), not unusual for a quiescent dwarf nova (Friend et al. 1988).

The TiO bands at $\lambda\lambda$7150 and 7650 Å revealed this CV's red star (see Fig. 1). We assumed that this secondary had an absolute magnitude of an M dwarf, and then used its measured dilution to find the absolute magnitude for CZ Ori. For the spectral type and orbital period found below, the secondary would lie on the empirical ZAMS of Patterson (1984), which justifies our assumption that it is a dwarf. To measure its spectral type, spectra of M dwarfs of known spectral type, spanning types M0–M6.5 in the system of Kirkpatrick, Henry & McCarthy (1991), were normalized and fitted to the composite spectrum of CZ Ori. Minimization of χ^2 for these fits (see Mukai & Charles 1986) showed that an M2.5 $\pm$ 1.0 spectrum left the smoothest disc spectrum (Fig. 1, middle trace).

After correction for the star's red colour (Bessell 1986), the effective average wavelength of Kron–Cousins R for an M2.5 dwarf is λ6750 $\pm$ 100 Å. The red star contributes 36 per cent of the light at λ6750 $\pm$ 100 Å, and an M2.5 dwarf has an absolute magnitude in $R_{\rm KC}$ of 9.62 (Bessell 1991). Therefore, in quiescence, CZ Ori has an absolute magnitude in $R_{\rm KC}$ of 8.51 $\pm$ 0.98.

This procedure avoided error in absolute spectrophotometry due to slit losses, but, to turn this absolute magnitude into a distance, this error could not be avoided. Assuming an accurate absolute flux level at λ6750 Å of 1.0×10^{-15} erg cm^{-2} Å^{-1} s^{-1}, an M2.5 dwarf with the observed fraction of the light would have $R_{\rm KC}=16.7$, and a distance of 260 $\pm$ 110 pc. Warner (1987) estimated a distance of 300 pc, based on

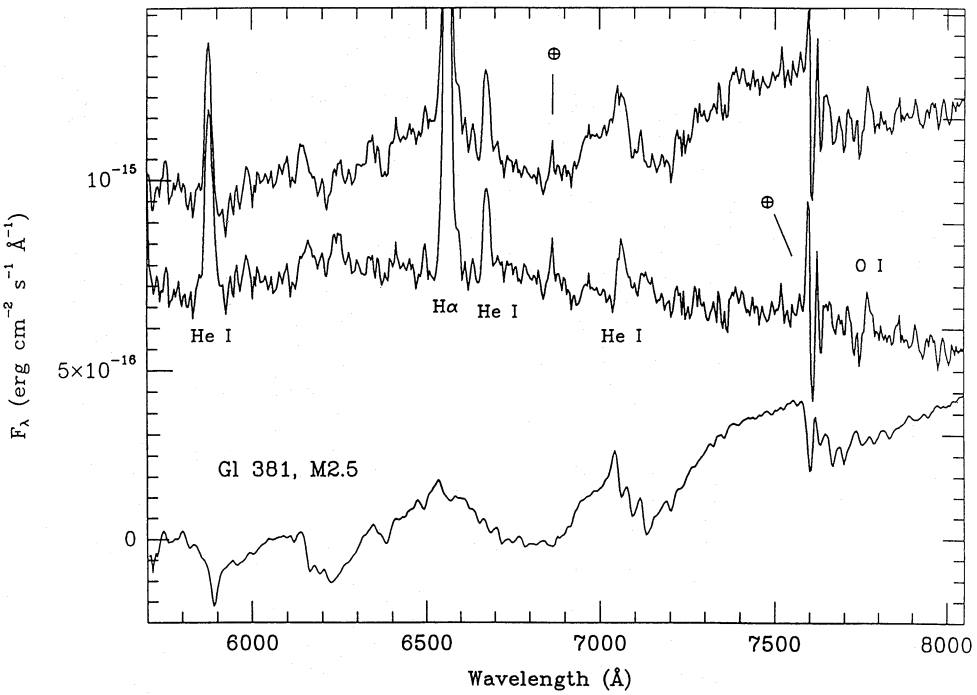

Figure 1. (Top) Average of the 10 spectra of CZ Ori from 1989, comprising a 100-min exposure time. A hot stellar spectrum was used to map and remove the telluric absorption, with some residual absorption near $\lambda\lambda$6870 and 7600 Å. (Middle) This is an average spectrum with a scaled M2.5-dwarf spectrum subtracted (see text). This should represent the spectrum of the low-luminosity disc alone, although spectrophotometric error may account for the down-turned slope. (Bottom) Scaled M2.5-dwarf spectrum, displaced downward by 1.7×10^{-16} erg cm^{-2} Å^{-1} s^{-1} for clarity.

correlations between outburst magnitudes and an assumed P_{orb} of 4.0 h.

During both epochs, the Hα emission line was unusually narrow, for a dwarf nova. We measured velocities for the 1988 spectra with a Gaussian separation of 970 km s^{-1}, and calculated a periodogram (Fig. 2, top). It showed two likely aliases, corresponding to periods of 4.32 and 5.25 h. The artificial sinusoid test produced a similar periodogram, including the spuriously high peaks at the low frequencies below 3 cycle d^{-1} (Fig. 2, bottom). Trying various Gaussian separations to maximize K_{em}/σ, we found that the optimal separation was 750 km s^{-1}. The alias at 5.25 h fitted a sinusoid better (see Table 1a and Fig. 3), so we adopted this alias as the orbital period. Using $\sigma = 14.5$ km s^{-1} for the Monte Carlo analysis, we calculated the correctness likelihood and the discriminatory power; both exceeded 98 per cent. Therefore, in over 50 identically sampled observing runs, noise in the velocity curve would have only once caused

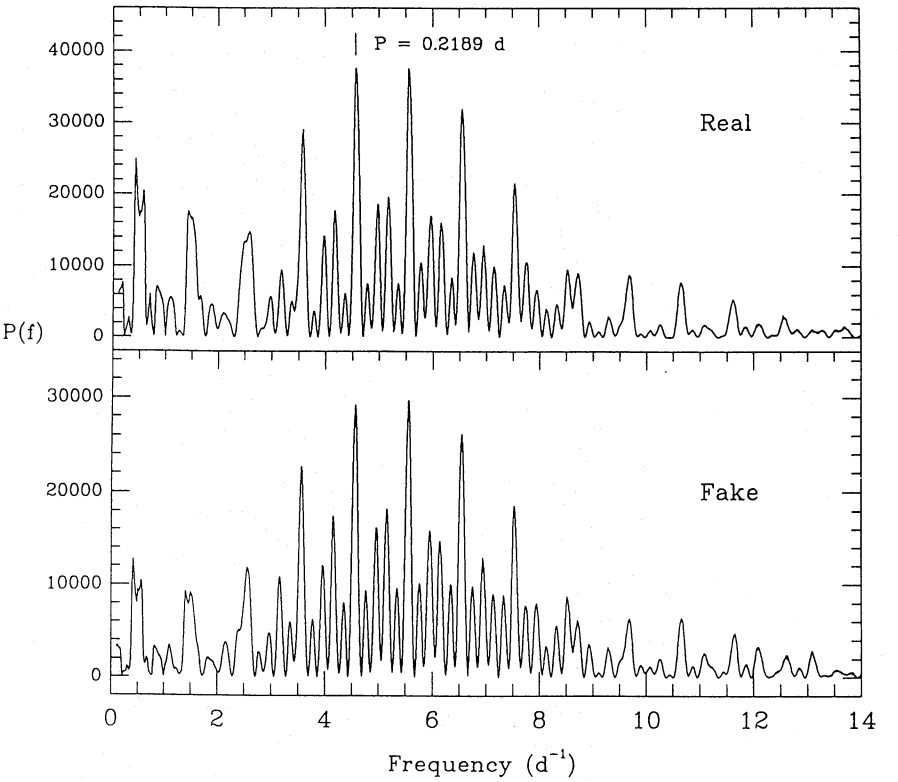

Figure 2. (Top) Periodogram for Hα velocities for CZ Ori, 1988 January spectra. The two highest peaks correspond to aliases at 4.32 and 5.25 h. The favoured alias, at 5.25 h, is marked. (Bottom) Periodogram for an artificial sinusoid given the same parameters as the orbit (see Table 1a), with $\sigma = 14.5$ km s^{-1} and sampled in time identically to the data. This shows that the shape of the periodogram results only from how the data are sampled; the noise at low frequencies (<3 cycle d^{-1}) is spuriously prominent. The two most likely aliases have nearly equal height, even though the one at 5.25 h fits a sinusoid better (see Table 1a).

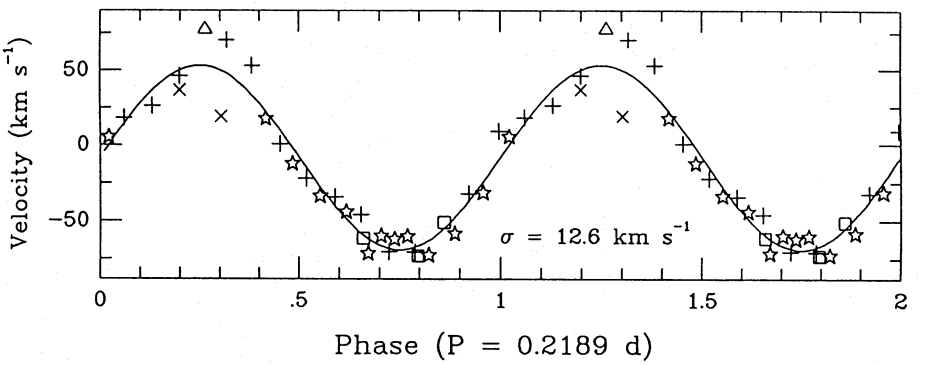

Figure 3. Fit to a sinusoid of the 1988 January velocities of CZ Ori measured from Hα. All velocities are plotted twice for continuity. Here we sample the line cores, which do not change through an outburst and so allow determination of the orbital period. The sinusoid's other parameters (see Table 1a) vary considerably from before to after the outburst. To show this, we have used different symbols for different nights: HJD − 2440000 + 7167: crosses; 7169: diagonal crosses; 7170: squares; 7171: triangles; 7172: five-pointed stars.

another alias, most likely the one at 4.32 h, to have had a better fit to a sinusoid.

The preferred alias also agrees with the orbital period determination of Spogli & Claudi (1994), although we suspect their errors are larger than claimed, since their time series involved an interpolation over 72 d. We calculated likelihood ratio tests for their radial velocities before and after this gap, and both showed that the gap was over three times longer than either series could be extrapolated over while accumulating an error in period of less than one cycle. We also found the series before and after the gap to have periods of 0.2126 ± 0.0018 and 0.2183 ± 0.0024 d, respectively.

3.2 Outburst

On 1988 January 7.46 UT, CZ Ori was quiescent; on January 8.34 UT, it was found in outburst. After a rapid transition back to an emission spectrum, on January 10.36 UT the continuum was still strong ($I_{H\alpha}/I_{cont} = 1.45$). CZ Ori was back near quiescence by January 12.29 UT. This therefore was a short-duration outburst.

We measured K_{em} and γ_{em} before and after the outburst by fitting sinusoids, with the orbital period fixed, to the velocities of January 7 and 9, respectively (see Table 1a). To 90 per cent confidence, K_{em} decreased in the line core. The dwarf novae SS Cyg (Robinson, Zhang & Stover 1986) and IP Peg (Hessman 1989) have also shown K_{em} decreasing immediately after outburst maxima. This decrease is thought to be from a narrow emission-line component from the illuminated red star. Also, γ_{em} became somewhat bluer in the line wings, but only to 68 per cent confidence.

3.3 Discussion

Supposedly, periodogram analysis is equivalent to least-squares fitting (Scargle 1982). Why, then, does CZ Ori's periodogram not show a peak at the orbital period that towers over all others? The artificial sinusoid test shows that the culprit was the sampling: since these data were so unevenly sampled about the orbital phase, the mean of the data was not the mean of the fit. This equality is assumed implicitly in the derivation of the periodogram (Lomb 1976; Scargle 1982), however. Correction of the periodogram is outside the scope of this paper, although a linear least-squares spectrum may not suffer from this problem, provided one fits

$$y(t) = A \sin \omega t + B \cos \omega t + C$$

to the data at each trial period, where $C \neq 0$, necessarily. This was no problem in the analyses for V1193 Ori and BZ UMa, as their radial velocity curves were thoroughly sampled in phase.

Our orbital period agrees within 3 per cent with the period predicted by the relation of Bailey (1975), as calibrated by Szkody & Mattei (1984). This relation is a linear correlation between outburst decline time and orbital period and is among the clearer correlations between an outburst statistic and an intrinsic CV property. So far, this relation has successfully predicted the orbital periods of all the dwarf novae that Szkody & Mattei (1984) applied it to (AR And: Szkody 1985; X Leo: Shafter & Harkness 1986; KT Per: Ratering, Bruch & Diaz 1993), to within 10 per cent. It may arise from the maximum radius a disc can attain during an outburst, as affected by tides and Roche geometry (Smak 1984), which are set by the orbital period. A disc of a certain maximum size may take a certain amount of time to lose its excess heat. This relation deserves more thorough theoretical investigation.

4 V1193 ORIONIS

V1193 Orionis, also called Hamuy's Blue Variable, was discovered by M. Hamuy while making a photometric sequence. Maza & Hamuy (1986) reported $V = 14.08$, $B - V = 0.05$ and $U - B = -0.82$, with V varying by 0.3 mag. Hamuy & Maza (1986) gave a finding chart. Filippenko & Ebneter (1986) described a spectrum with 'relatively strong Hα and Hβ emission lines superposed on a nearly featureless continuum'. Bond et al. (1987) found an irregular flickering of peak-to-peak amplitude of over 0.15 mag. They also found a nearly continuous spectrum showing weak emission inside a broadened, shallow Hβ absorption line, and so classified V1193 Ori as a nova-like star similar to UX UMa. Warner & Nather (1988) found rapid flickering and unusually high amplitude, 0.25 mag, in 3.6 h of high-speed photometry. No orbital photometric modulation or eclipses were obvious in their light curve. They likened V1193 Ori to the brightest CV, IX Vel (= CPD $-48°$ 1577), another UX UMa star with rapid flickering, although of lower amplitude (Williams & Hiltner 1984).

4.1 Spectrum and orbit

The average of our spectra of V1193 Ori from 1989 (see Fig. 4) showed an Hα line twice as high at its peak as its surrounding continuum. Slight absorption wings flanked Hβ and He I λ5876 Å, verifying this object's classification as a UX UMa star (Warner 1976). Other He I lines were weakly present in emission (see Table 2a). Aside from the red absorption wing of He I λ5876 Å being slightly stronger than the blue wing and suggesting the presence of Na D, we saw no obvious sign of the red star, which was overwhelmed by the $\alpha = -2.77 \pm 0.01$ power-law continuum.

Owing to extreme line-wing variations, particularly of the red wing, we needed to measure close to the line core to obtain the best sine fit. We measured velocities from the 1989 spectra with a Schneider–Young convolution of 690 km s^{-1} FWHM, and calculated a periodogram (see Fig. 5, top). The most likely period was 3.96 h, and both Monte Carlo statistics exceeded 99 per cent, making the alias choice secure. The peculiar form of the periodogram resulted only from the sampling, as an artificial sinusoid test showed (Fig. 5, bottom), which used the deduced orbital parameters and added random noise of $\sigma = 17.2$ km s^{-1}.

Upon rebinning the spectra in velocity space and co-adding into 12 bins about the orbital phase, to reduce noise from random fluctuations, the best-fitting sinusoid for 1988 (see Fig. 6 and Table 1b) fitted better than any achievable with the 1989 velocities. While we did measure the 1988 velocities with the Shafter algorithm, we could not find an optimum Gaussian separation for the 1989 velocities, since K_{em}/σ reached a maximum in the innermost line core. This was only partly because of the resolution difference: the line profile

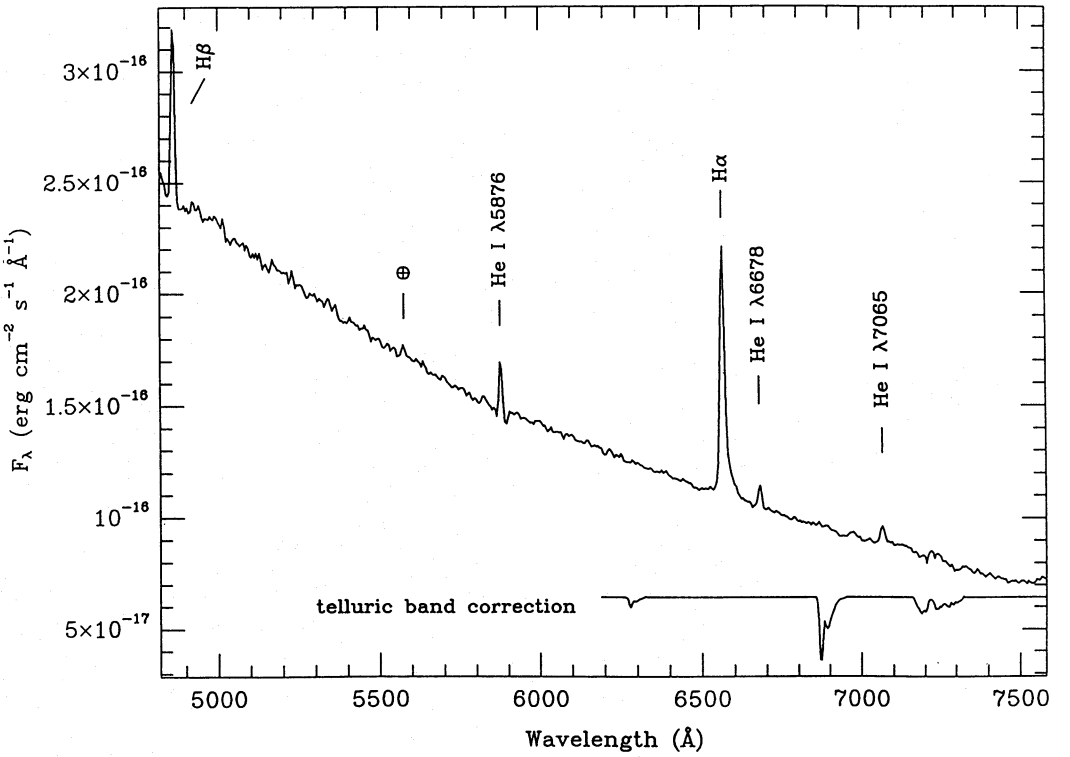

Figure 4. Average of the spectra of V1193 Ori from 1989, comprising over 5.8 h of exposure time. Night-sky lines were subtracted, with some residual emission at λ5577 Å. A hot star's spectrum was used to map and remove the telluric absorption bands, traced below. The red wing of Hα is variable in profile (see Fig. 7).

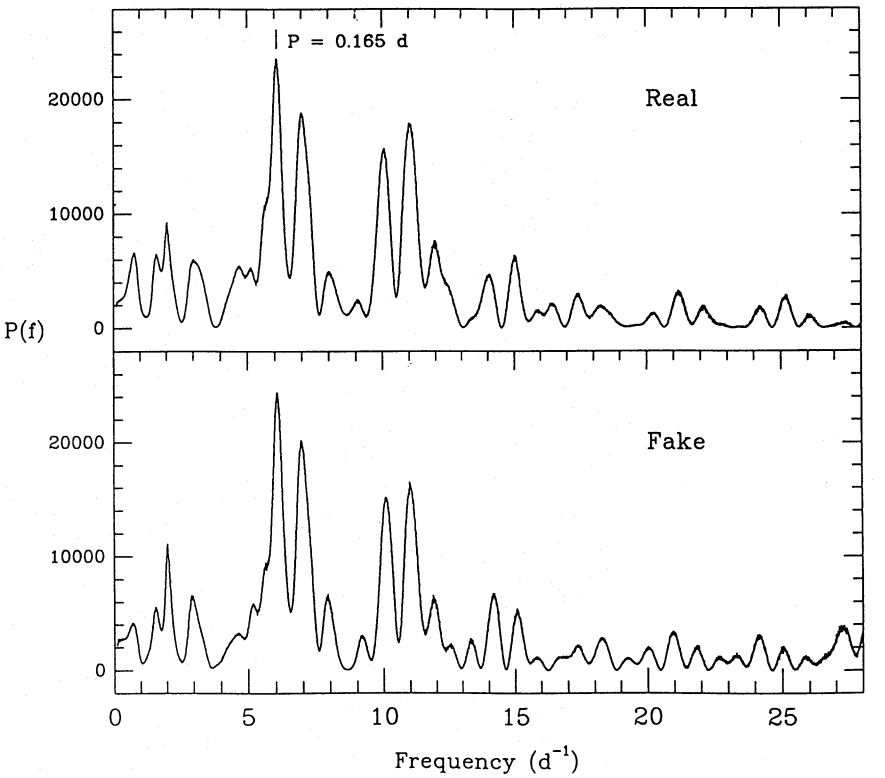

Figure 5. (Top) Periodogram of velocities of V1193 Ori from 1989 November. (Bottom) Identically sampled artificial sinusoid with the derived orbital parameters and random noise with $\sigma = 17.2$ km s^{-1} added. The similarity between real and fake periodograms shows that the periodogram's strange shape results from the sampling only.

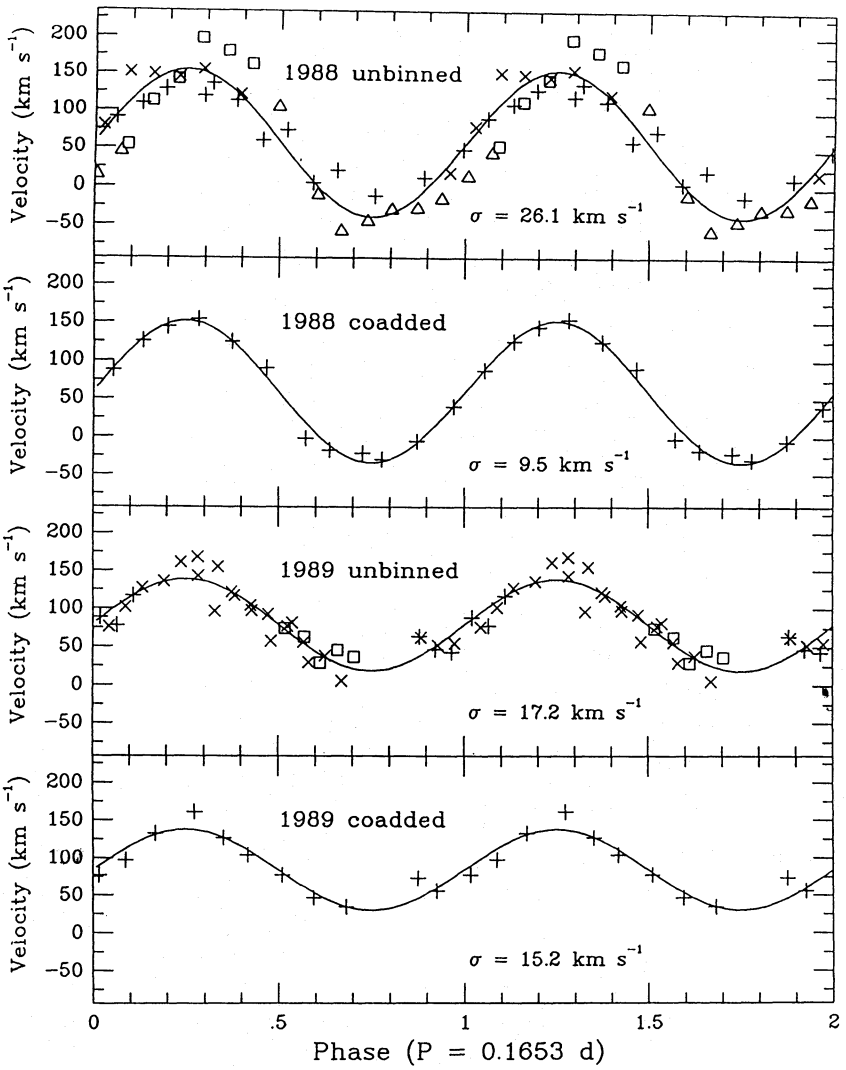

Figure 6. Sinusoid fits for radial velocities of the Hα line core of V1193 Ori (see also Table 1b). All data are plotted twice for continuity. (Top) For 1988, different nights plotted with different symbols: for HJD − 2440000 + 7169: crosses; 7170: diagonal crosses; 7171: squares; 7172: triangles. (Middle-top) Fit to velocities measured from spectra co-added into 12 phase bins, to decrease noise. (Middle-bottom) For 1989, different nights plotted with different symbols: for HJD − 2440000 + 7842: crosses; 7843: diagonal crosses; 7844: squares. (Bottom) Co-added into phase bins, as above: note the changes in K_{em} and γ_{em}, from epoch to epoch.

was genuinely changing more in 1989, since, all else being equal, line profiles should appear to vary more in higher resolution spectra.

In 1988 (Fig. 7, left), the Hα line profile varied about the orbital cycle in a way similar to that seen in RW Tri and UX UMa (Honeycutt, Kaitchuck & Schlegel 1987) and in IX Vel (Beuermann & Thomas 1990). This is thought to result from a narrow emission line component raised on the red star by disc illumination. Even though the Hα velocities did not shift in phase from the line core to the line wings, the Hα equivalent width varied nearly oppositely in phase to the velocity (see Fig. 8).

The cyclic variation of Hα in 1989 was peculiar (Fig. 7, right). Gone was any indication of illumination, with the equivalent width varying erratically with phase (Fig. 8). Pronounced line profile variations occurred in the red wing around $\phi = 0.2$ and 0.8, which distorted the grand-sum line profile (Fig. 4). In 1989, K_{em} was significantly smaller (see Table 1b). Also γ_{em} was redder, perhaps from the strong red wing flaring, but we caution that the velocity scales for two different runs may have been systematically consistent to only about 20 km s^{-1}, as experience with cross-correlating radial velocity standards has shown. Such shifts in the velocity scale would not affect K_{em}, however. Whatever its cause, this epoch-to-epoch change in K_{em} casts serious doubt on whether CV emission lines trace the orbital motion of the white dwarf.

4.2 Discussion

A ZAMS M2 red star could fit inside the Roche lobe of V1193 Ori (Patterson 1984). By scaling an M2 spectrum and adding it to the spectrum of V1193 Ori, we estimate that the red star contributes less than 5 per cent of the flux at λ6750 Å, otherwise the TiO bands would have become noticeable in Fig. 4. V1193 Ori should then have an absolute magnitude

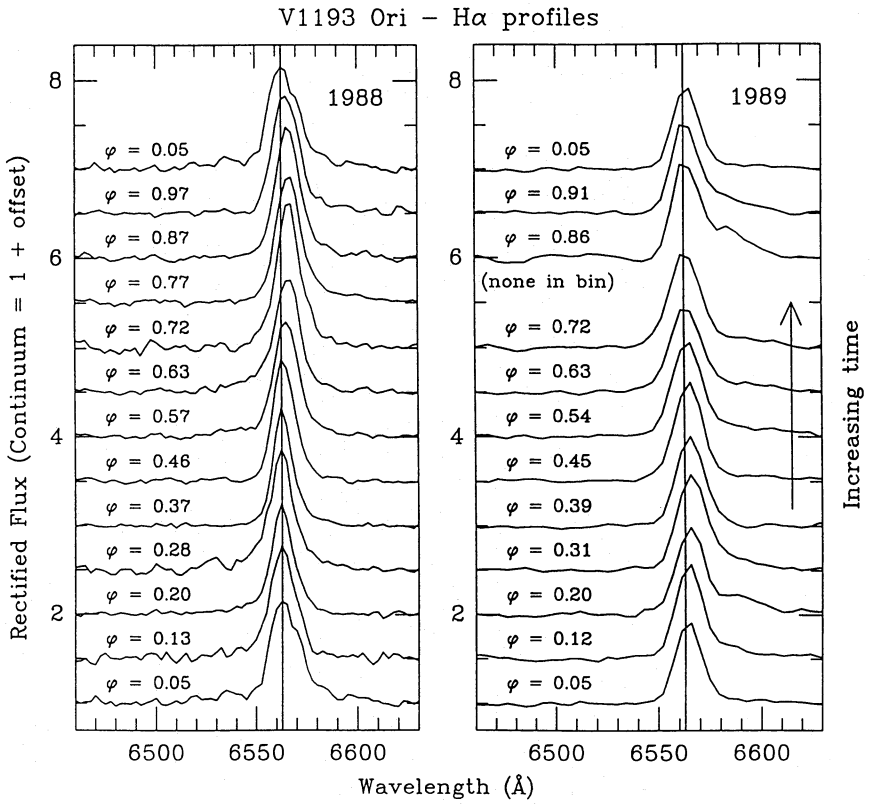

Figure 7. Line profile changes in V1193 Ori, for 1988 January (left) and 1989 November (right). Differences between the two epochs cannot be resolution effects alone, as seen by the behaviour of the red wing.

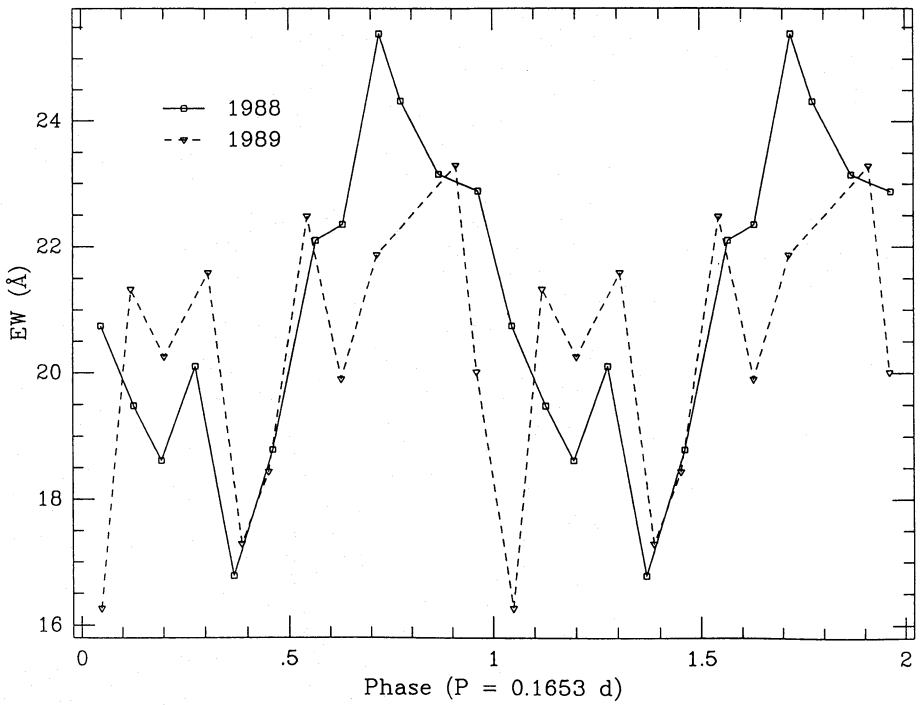

Figure 8. Hα equivalent width versus phase for V1193 Ori, for both epochs. The 1988 equivalent widths show a sinusoidal variation, $\sigma = 1.1$ Å, of amplitude 3.2 Å and average 21.2 Å. Phase zero is at $\phi = 0.546 \pm 0.022$, or $180° + 17° \pm 8°$ out of phase with the radial velocity curve. This suggests illumination of the red star by the disc (and perhaps bright spot: see Beuermann & Thomas 1990; Davey & Smith 1992). The 1989 spectra show only erratic equivalent width variations, $\sigma = 2.3$ Å, with an average of 20.5 Å.

in R_{KC} of <5.9. At a flux level of 3.5×10^{-15} erg cm^{-2} Å^{-1} s^{-1}, this implies a distance limit of >470 pc.

High-speed photometry (Bond et al. 1987; Warner & Nather 1988) shows that V1193 Ori flickers rapidly, with a large amplitude that could mask shallow eclipses. Unfortunately, too, the published time-resolved photometry covers just enough phase to miss an eclipse, if present.

The 1989 Hα red wing variations are reminiscent of those of AM Her (Crosa et al. 1981), with its high γ_{em} and broad line wings. There is no corresponding strong blue wing on the other side of the orbit, though, and V1193 Ori's red wing is strongest twice per orbit. It is unlikely anyway that V1193 Ori is a magnetic CV, since it shows neither obvious coherent optical pulsations, nor strong He II λ4686 Å (Bond et al. 1987), nor X-rays detected by *HEAO-1* (Wood et al. 1984; Silber 1992).

The red wing spike in the 1989 spectra occurred twice per orbit, at $\phi=0.2$ and 0.8. Interestingly, Livio (1993) suggests that the stream–disc interaction may cause thickenings of the disc at azimuths corresponding to just this combination of orbital phases, assuming superior conjunction of the white dwarf occurring at $\phi=0.0$. Various CVs and X-ray binaries show peculiar behaviour at these two orbital phases, such as in the absorption in the X-ray light curves of coronal sources (White & Holt 1982) and some dwarf novae (Mason et al. 1988), and in the two bright spots on the disc rim of many dwarf novae (Wood, Hessman & Fiedler 1990; Livio 1993 and references therein).

5 BZ URSAE MAJORIS

BZ UMa was serendipitously discovered in outburst by Markarian (1968), who gave a finding chart and coordinates, as did Bruch et al. (1987). The Palomar–Green survey (Green, Schmidt & Liebert 1986) listed it as PG 0849+580. The compilation of Green et al. (1982) of CVs found by this survey showed and described a blue spectrum. The Balmer jump was in emission, the broad Balmer and He I emission lines were doubled, and a weak, broad He II λ4686-Å emission line was blended with C III/N III $\lambda\lambda$4640–4650 Å. Bruch (1989) also presented a spectrum and described it as 'a textbook example for a spectrum of a dwarf nova'. The lines are unusually strong, though: we found equivalent widths for Hα of about 200 Å (see Tables 2a and b).

BZ UMa has very infrequent outbursts, with mean intervals longer than 5.2 yr (Wenzel 1982). Recent outbursts were in 1990 July (Schmeer 1990), 1991 April and 1992 October (Mattei 1992) and 1993 April (Mattei 1993), and, although there have been reports of others (Hurst & Lubbock 1988), the last confirmed outburst before this was in 1975 (Mattei 1989, AAVSO observations, private communication). Dwarf novae with interoutburst intervals exceeding 400 d generally only have outbursts with the amplitudes and durations of the superoutbursts of the SU UMa stars (Warner 1987; Ritter & Kolb 1994), and BZ UMa is no exception. These outbursts are slow, lasting 10–20 d, with large amplitudes of $\Delta V\approx6$. Superhumps, the other defining property of the SU UMa stars, have eluded detection in BZ UMa but may well exist; to our knowledge, there has been no published time-resolved photometry of an outburst.

Dwarf novae with rare outbursts are sometimes called WZ Sge stars, after a CV with mean interoutburst intervals of 32.5 yr. O'Donoghue et al. (1991) reviewed these, showing that they appear to have few physical differences from the SU UMa stars. Wenzel (1982) called BZ UMa an intermediate case between WZ Sge and U Gem, because its outbursts are rare, but its spectrum (Figs 9–11, Tables 2a and b) more resembles that of U Gem (Oke & Wade 1982). WZ Sge shows Balmer lines in emission with broad absorption wings, perhaps from its white dwarf, and no trace of a red star (Williams 1983).

5.1 Spectrum and red star

In our spectra of BZ UMa (Fig. 9 and Table 2b), Hα was much broader than in CZ Ori or V1193 Ori. The other Balmer and He I lines were also in broad, strong emission, with no trace of absorption wings. Hβ was double-peaked, with a peak-to-peak separation of 560 ± 50 km s^{-1}. In the higher resolution 1988 spectra, not shown, He I λ5876 Å, λ6678 Å and λ7065 Å were double-peaked, with peak-to-peak separations of 1000, 950 and 1100 ± 50 km s^{-1}, respectively. He II λ4686 Å was in weak, broad emission and the presence of the C III/N III blend at $\lambda\lambda$4640–4650 Å was not obvious.

With the methods of Section 3.1, we fitted and subtracted an M5 dwarf from the red spectrum, not quite perfectly (see Fig. 10). Use of an M6 dwarf left even more noticeable residual traces of the red star, as did earlier types, so we inferred a spectral type of M5.5 ± 0.5. Again our assumption that the red star is a dwarf was borne out, since an M5.5 star on the empirical ZAMS of Patterson (1984) would just fill the Roche lobe of a CV with the orbital period we found (see Section 5.2). The fraction of light from the red star at λ7000 Å was 4.5 per cent. We estimated for BZ UMa a quiescent absolute magnitude in R_{KC} of 10.69 (+0.66/−0.85). At the flux level of 8.7×10^{-16} erg cm^{-2} Å^{-1} s^{-1} through the narrow slit at λ7000 Å, this implied a distance of 110 (+44/−51) pc, probably overestimated by <30 per cent.

The O I λ7773-Å feature was in strong emission and appeared doubled even in our low-resolution spectra, with a peak-to-peak separation of 840 ± 70 km s^{-1}. Na I λ8190 Å and He II λ8236 Å were not obviously present, overwhelmed by perhaps the strongest 'λ8200-Å bump' yet seen in any CV (Friend et al. 1988). This feature could not have been from telluric water vapour absorption, since it remained both with and without the telluric band correction (see Fig. 11). The Paschen and Ca II lines were in strong emission and double-peaked (see Fig. 11). The Ca II lines had separations ranging from 600 to 700 km s^{-1}, and the Paschen lines ranged from 600 to 850 km s^{-1}, although blending made these hard to measure.

The λ8200-Å bump, thought to be unresolved Paschen lines in emission, was all the more unusual as it is normally seen in luminous CVs (Friend et al. 1988). Then again, BZ UMa has strong emission lines of most kinds. This λ8200-Å bump made it difficult to find, much less fit, the continuum just to the red of λ8200 Å, and this complicated precise spectral typing of the red star by measuring the flux deficits of the TiO bands (Wade & Horne 1988). We tried this and it gave a spectral type of M6.5+, clearly too red: we caution against trusting this method to excessive precision. Contamination by emission features may explain the unexpected illumination asymmetry found in maps of CV red stars' Na I λ8190-Å absorption by Davey & Smith (1992).

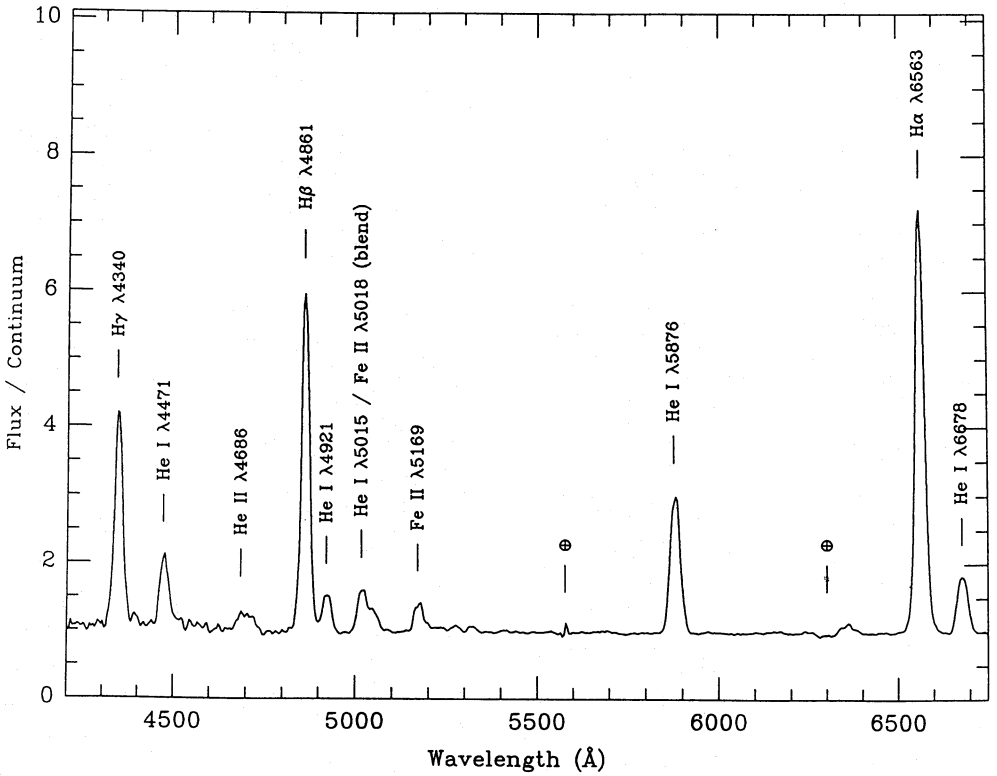

Figure 9. Rectified sum of the 1989 March spectra of BZ UMa, comprising over 24 h of exposure time. The emission lines are unusually strong, Hα having an equivalent width of nearly 200 Å. Spurious features at $\lambda\lambda$5577 and 6300 Å are from bad night-sky line subtractions.

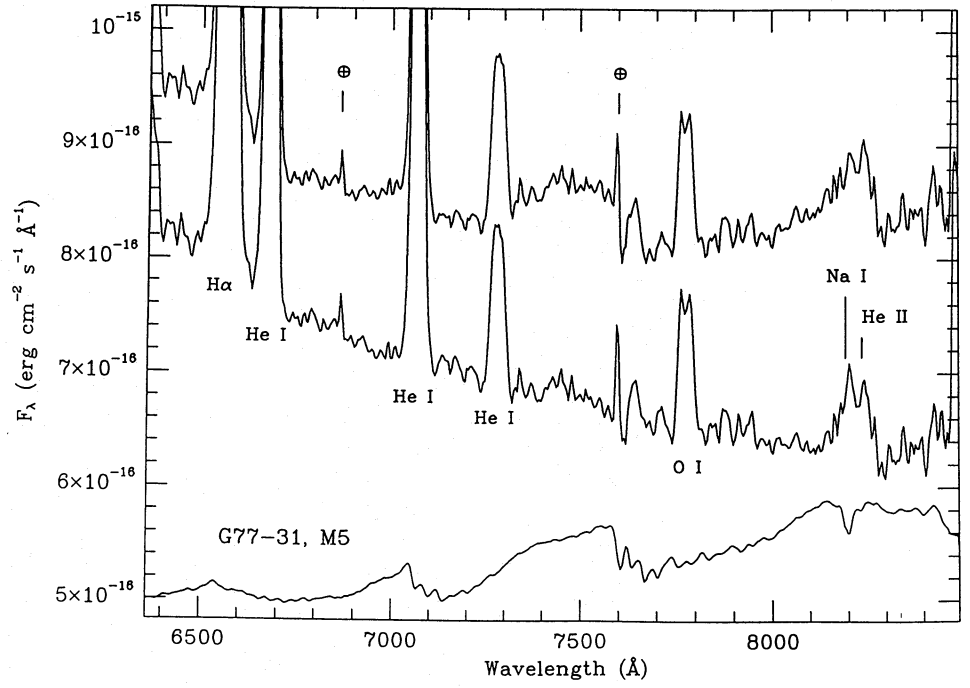

Figure 10. (Top) Average of the 1991 spectra of BZ UMa, in the red region and sky-subtracted. A low-Z sdF spectrum was used to measure the profiles of the telluric atmospheric bands, subsequently scaled and subtracted, with some residual absorption near $\lambda\lambda$6870 and 7600 Å. (Middle) Same spectrum, with a scaled M5 dwarf spectrum subtracted (see text). The strong anomalous emission bump at λ8200 Å obscures any trace of the Na I or He II features. This deconvolved spectrum is displaced downward by 1.4×10^{-16} erg cm^{-2} Å^{-1} s^{-1} for clarity. (Bottom) Scaled M5 dwarf spectrum, displaced upward by 6.4×10^{-16} erg cm^{-2} Å^{-1} s^{-1} for clarity.

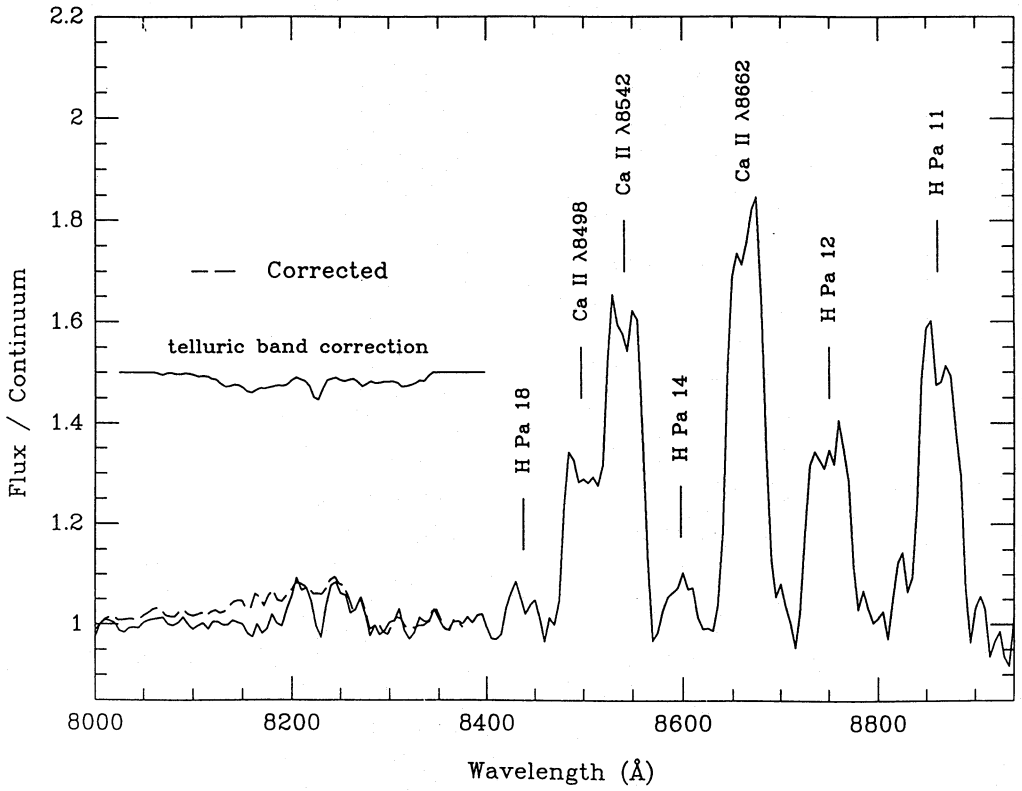

Figure 11. Rectified red end of the 1991 spectra, shown both corrected and uncorrected for telluric absorption. The bump at $\lambda 8200$ Å never goes away.

5.2 Orbit

Periodogram analyses of Hα velocities measured with both line-measuring algorithms showed a periodicity of 97.8 min. We took this to be the orbital period, since an *S*-wave was apparent in the Hα line profile, upon binning the 1988 spectra in phase about this period and co-adding them (see Fig. 12). The peak of this *S*-wave had a semi-amplitude $K_S = 300 \pm 50$ km s^{-1}. There was also an independent spectroscopic confirmation of $P_{\rm orb}$ by Claudi, Bianchini & Munari (1990), although they did not give many details.

To measure velocities of different parts of the Hα line, we used the double-Gaussian algorithm, to avoid the *S*-wave by measuring far into the line wings. In all cases (Fig. 13, top three panels), periodogram peaks appeared at low frequencies, below 10 cycle d^{-1}. These were not aliases of the orbital period, which clearly clustered at 1 cycle d^{-1} intervals about the orbital periodicity because the velocities were well-sampled in time. Neither could they have arisen from the sampling in any way: an artificial sinusoid test, using the orbital period and parameters from a least-squares fit to the velocities, showed no excess power at low frequencies (Fig. 13, bottom panel). These peaks had higher significance than those of the orbit, except when evaluated using velocities measured from the core of the line, and they increased in power farther out into the wings.

These low-frequency variations appeared to be sinusoids, since they made discrete peaks in the periodogram, not bands or smears. The most significant peaks corresponded to periods of 17.8 and 38.4, both accompanied by patterns of 1 cycle d^{-1} aliases from the day–night cycle (Fig. 14, bottom). Judging from the width of the oversampled periodogram peaks of about 0.1 cycle d^{-1}, $Q \equiv f/\Delta f \approx 15$ for the 1989 quasi-periodicities. However, our observations sampled only 9.4 or 11.3 long periods, over a 7-d baseline, so this estimate was limited by frequency resolution. We adopted a separation of 1370 km s^{-1} for the remaining analysis, to compromise between the core velocities, which followed the orbit but may have been contaminated by the *S*-wave, and wing velocities, which exhibited these mysterious low-frequency variations most strongly.

We fitted a least-squares sinusoid to the 17.8-h velocity variation of the orbit, subtracted it from the radial velocity curve and calculated a periodogram (Fig. 14, top). We also did this for the 38.4-h variation (Fig. 14, middle) and show the resulting fit parameters in Table 1(c). In both cases, the measured orbital variation did not change significantly. After subtracting both long periodicities from the original velocities, the resulting periodogram looked like the artificial sinusoid's (see Fig. 15). A third quasi-periodic variation at 3.13 h, at the threshold of significance and perhaps only noise, could be fitted and subtracted as well. Subtraction of sinusoids fitting these low-frequency quasi-periodicities from the radial velocity curve gave it a much better fit to a sinusoid, halving σ at least (see Fig. 16).

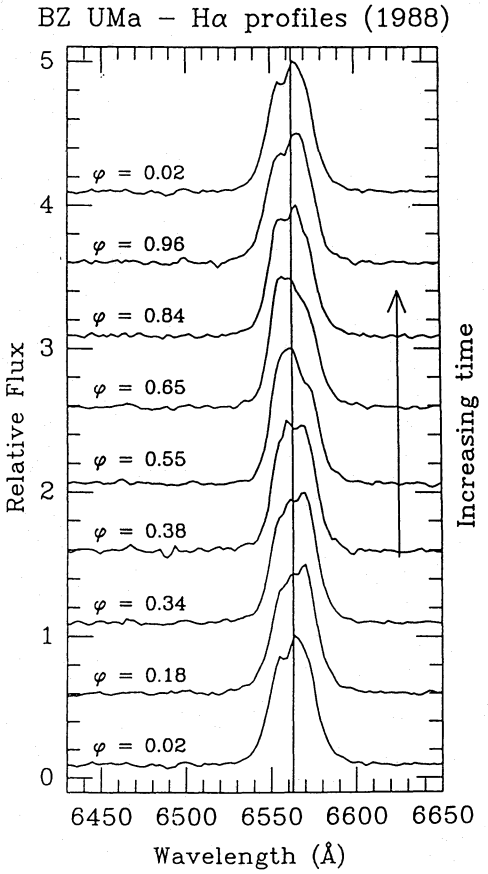

Figure 12. That the 97.8-min periodicity is the orbital period is shown by this *S*-wave in the profile of Hα. These spectra are binned over a 97.8-min period, co-added to reduce noise, and rectified, normalized in height and given arbitrary offsets in height, to avoid overlap.

5.3 Blue and infrared time-resolved photometry

Four hours of time-resolved CCD photometry by Kaluzny (1986) showed flickering variations in B of about 0.1 mag, with BZ UMa at $B=17.8$, much fainter than the $B=15.3$ seen by Green et al. (1982). With a periodogram analysis down to the Nyquist limit of 90 s, we found no obvious coherent optical pulsations to indicate a magnetic white dwarf. With no obvious eclipses, we could still place limits on the orbital inclination i, although, since the disc radius is uncertain, one must be content with a limit precluding white dwarf eclipses. For grazing eclipses, assuming the red star fills its Roche lobe,

$$\cos i = \frac{R_L}{a} = \frac{0.49q^{2/3}}{0.6q^{2/3} + \ln(1+q^{1/3})},$$

using the approximation of Eggleton (1983), where $4\pi R_L^3/3$ is the volume of the lobe, a is the semimajor axis of the circular orbit and q is the binary mass ratio, $q \equiv M_2/M_{WD}$, where M_{WD} is the white dwarf mass and M_2 is the red star mass. We took the red star mass to be 0.13 $M_\odot$, from the approximation $M_2/M_\odot = 0.38\,(P_{orb}/4\ \mathrm{h})^{1.22}$ (Patterson 1984). The white dwarf mass was more problematical, difficult to measure even in the best circumstances (Wade & Horne 1988), so we considered the entire plausible range of masses, from 0.3 to 1.4 $M_\odot$. These values constrained i to be $<72°$ to 78°, respectively, with $i<76°$ for $M_{WD}=0.65\ M_\odot$. Using the gas stream's circularization radius (Plavec & Kratochvil 1964; Livio 1994) as a minimum disc radius, we obtained $i<68.^\circ4$, 73° and 71°, respectively.

Szkody & Feinswog (1988) obtained *JHK* colours and a *J* light curve, based on just over 3 h of continuous observations. They found a period of 107 ± 11 min, which agrees with ours, although they attributed this variation to ellipsoidal variations of the red star and so derived an orbital period twice as long as this. Again, no eclipse was obvious. With the *JHK* magnitudes of Szkody & Feinswog (1988) and flux-ratio diagram method of Berriman, Szkody & Capps (1985), we estimated with our revised orbital period that the red star contributes <25 per cent of the light in K, and so the red star has $K>15.7$. Using the photometric parallax method of Bailey (1981), recalibrated by Ramseyer (1994), and assuming an M5.5 red star of radius 0.13 $R_\odot$ (see Section 5.1), we found a distance of >140 pc.

5.4 Discussion

A consistent picture of BZ UMa is emerging, of a dwarf nova with a very low accretion luminosity. This is shown by the infrequent outbursts, extremely strong emission lines, weak disc continuum and detectable X-ray emission (see below) and late-M secondary. The rare outbursts and short orbital period may explain why the outbursts have large amplitudes: they might all be tidally driven superoutbursts, so any outburst should be searched for superhumps. A surprise, perhaps only incidentally related to this picture, is its wandering radial velocity curve.

BZ UMa's radial velocity curve shows excess power at low frequencies. We are confident of having identified the orbital period, because an *S*-wave is superimposed on it. Periodograms show this power is most excessive in the high-velocity material, although the low-velocity material is also affected, since the whole Hα line shifts. We consider explanations for this curious behaviour.

(i) **Instrumental effects.** How the slit was illuminated could have introduced a velocity error, but this should have been unimportant in the red. Guiding errors should have been small, since the guiding TV camera was red-sensitive. Autoguiding for the 1989 run was nearly always accurate to within 0.1 arcsec, corresponding to a velocity error of <18 km s^{-1}, and was always accurate to within 0.2 arcsec. Seeing during this run was generally better than 2 arcsec, except for nights 5 and 6, on which it was 2.5 arcsec.

Measurement of velocities of the λ5577-Å night-sky line should have uncovered problems here, as well as with the wavelength scale or its stability, but none was found in the 1989 spectra (see Fig. 17). There was some shifting in this line, but it occurred on the diurnal time-scale, and its semi-amplitude was about 10 km s^{-1}. The semi-amplitude of the anomalous velocity variation exceeded 40 km s^{-1}. The standard deviation of the velocities measured from the λ5577-Å line was 7.4 km s^{-1}. That of the λ6300-Å night-sky line was 14.6 km s^{-1}, although experience shows that this line is usually less precise for this test, being surrounded by variable absorption. The standard deviation of the Hα velo-

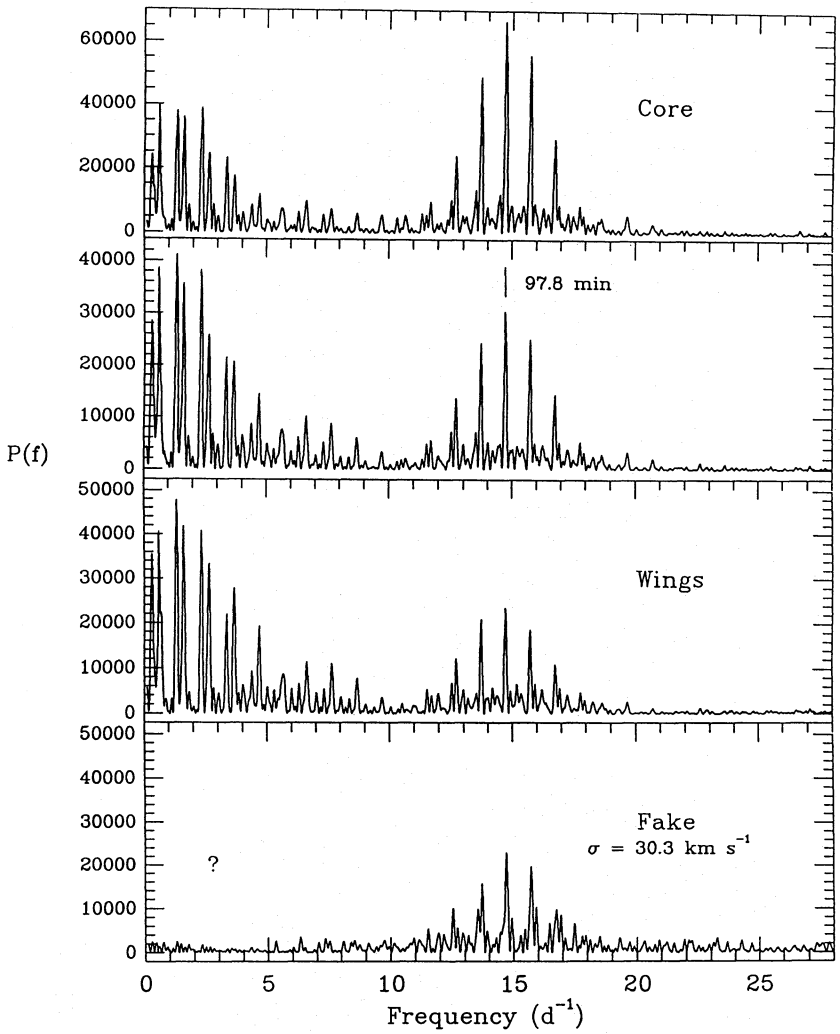

Figure 13. (Top and Middle-top, Middle-bottom) Periodograms of Hα velocities, measured by the double-Gaussian algorithm. Gaussian separations range from 690 km s^{-1} (marked Core), to 1370 km s^{-1}, to 2060 km s^{-1} (Wings). The low-frequency velocity variations become stronger in the line wings. (Bottom) Periodogram of an artificial ('Fake') sinusoid with parameters similar to the orbit's, given random noise with $\sigma = 30$ km s^{-1} and identical sampling in time to that of the real data. No low-frequency variations are present, so they cannot arise from the sampling of the time series.

cities, after the orbit is fitted and subtracted, was 37.9 km s^{-1} and without subtracting the orbit was 45.6 km s^{-1}.

Furthermore, one need not rely on statistics to see this effect. Every part of the cycle was manifest: night 1 showed a net decrease in γ_{em}, night 2 showed a smooth increase, night 5 showed a minimum and night 6 showed a maximum. If something was wrong due to atmospheric dispersion or spectrograph flexure, one might expect whatever effect to be similar from night to night. If something was wrong due to some mechanical failure in the instrument, one might expect the mysterious velocity variations to be erratic, not to vary smoothly, as on night 1 and especially night 2.

We also found anomalous velocity variations during two other epochs (see Fig. 18). Neither run had the frequency resolution of the 1989 run, but, even so, whenever a sinusoid with the orbital period was fitted to the radial velocity curve and subtracted from the radial velocities, rumbling of similar amplitude persisted. Curiously, this rumbling might have changed period (if indeed it was periodic) between epochs (see Table 1c). Since the wavelength scale for the 1989 spectra was calibrated to the red of Hα by only three neon lamp lines, we worried that our wavelength solution was in error, but since three different instrumental setups at different epochs showed some rumbling, it probably was not from the wavelength solutions.

BZ UMa's Hα emission line is very strong, so this effect was perhaps not entirely due to noisy velocity measurements. Besides, the anomalous variations in 1989 were probably not noise variations: when fitted to sinusoids, they could be subtracted without leaving a trace (see Figs 14 and 15).

Nevertheless, it is impossible to exclude categorically some unknown instrumental effect, but at least one other non-eclipsing CV, V795 Her (=PG 1711+336), has shown similar behaviour. These observations were taken with different instruments by Shafter et al. (1990), who noted line profile variations causing a noisy radial velocity curve. In one epoch, a low-frequency velocity variation was so strong that it completely masked this CV's orbit (Thorstensen 1986).

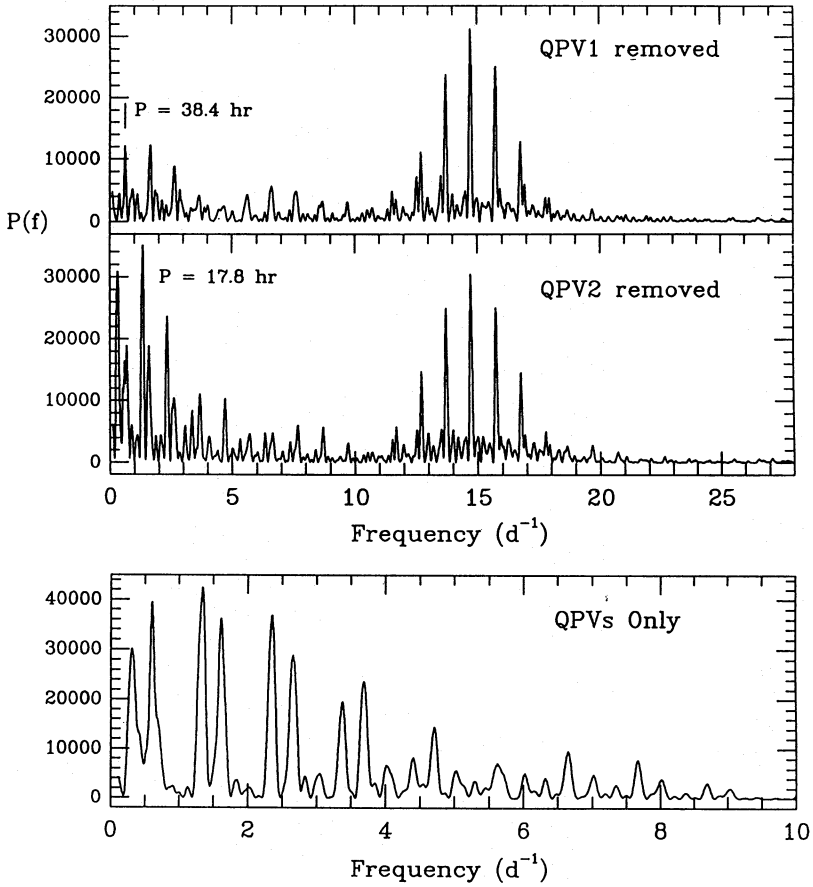

Figure 14. (Top, Middle) For velocities measured with a Gaussian separation of 1370 km s^{-1}, we fit low-frequency sinusoids to the velocities, subtract them and generate these periodograms. This suggests that at least two low-frequency quasi-periodic variations (QPVs) are present. (Bottom) Fig. 13, Middle-top, expanded to show only the low-frequency quasi-periodicities. We see at least two, attended by forests of 1 cycle d^{-1} aliases.

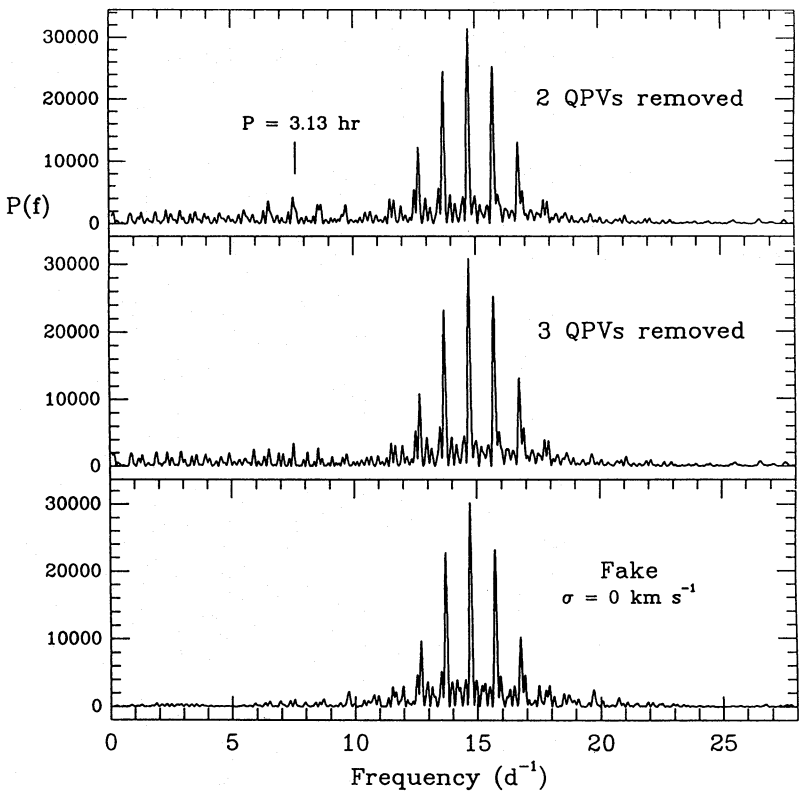

Figure 15. (Top) After subtracting both the strong low-frequency quasi-periodic variations from the velocities, another periodogram suggests that a weak third one is present. (Middle, Bottom) With three sinusoids subtracted, the periodogram strongly resembles that of a sinusoid with the orbital parameters (labelled 'Fake').

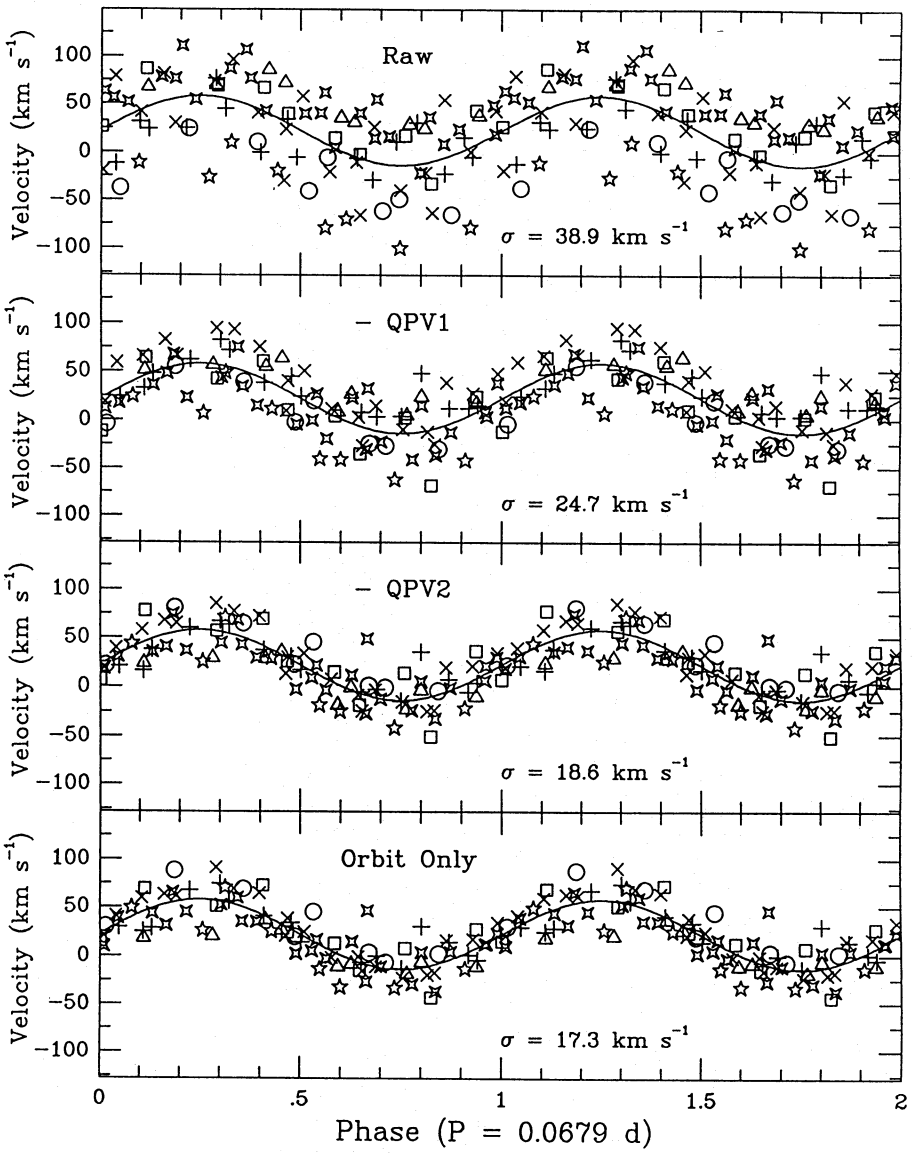

Figure 16. (Top) The radial velocities for BZ UMa, plotted about the orbital phase. All data are plotted twice for continuity, with different nights plotted with different symbols: for HJD − 2440000 + 7600: crosses; 7601: diagonal crosses; 7602: squares; 7603: triangles; 7604: five-pointed stars; 7705: four-pointed stars; 7607: circles. (Middle-top, Middle-bottom and Bottom) When low-frequency sinusoids, corresponding to the quasi-periodic variations, are fitted to and subtracted from the radial velocity curve, its fit to a sinusoid improves.

(ii) **A magnetic white dwarf.** Here, BZ UMa's inner disc would be disrupted into one or two columns that accrete on to the white dwarf's magnetic pole(s). The time-scale for this seems too long, and we find it difficult to explain more than one low-frequency quasi-periodicity in this way. Magnetic CVs have high-excitation optical spectra, unlike that of BZ UMa (see Williams 1983). BZ UMa also has negligible circular polarization (Liebert & Stockman 1980; Stockman et al. 1992). This possibility still should not be dismissed, however, since V795 Her has been suspected of harbouring a magnetic white dwarf (Shafter et al. 1990; see their figs 6 and 7). V795 Her is unusual for another reason: it is in the well-known CV period gap. This may contradict white dwarf magnetism, since it might be explained by an extreme mass ratio (Hameury, King & Lasota 1991). An extreme mass ratio may produce permanent superhumps (Patterson & Richman 1991), giving the observed photometric variability, although the stability of these photometric variations observed by Zhang et al. (1991) may be difficult to explain in this way.

If the rumbling of BZ UMa does indicate white dwarf magnetism, it may be possible to detect coherent optical oscillations with high-speed optical photometry. BZ UMa is an X-ray source (1H 0849 + 578; Silber 1992), albeit a faint one ($f_X = 0.3$ μJy at 5 keV, assuming a Crab-like spectrum; Wood et al. 1984), so that, if magnetic, it may have coherent X-ray oscillations.

(iii) **Disc oscillations.** Thorstensen (1986) found a 0.6157-d periodicity in the radial velocity curve of V795 Her. Its strongest 1 cycle d^{-1} alias, 1.60 d, is close to the beat period between the orbital and photometric periods (Shafter et al. 1990). Several authors have considered waves in accre-

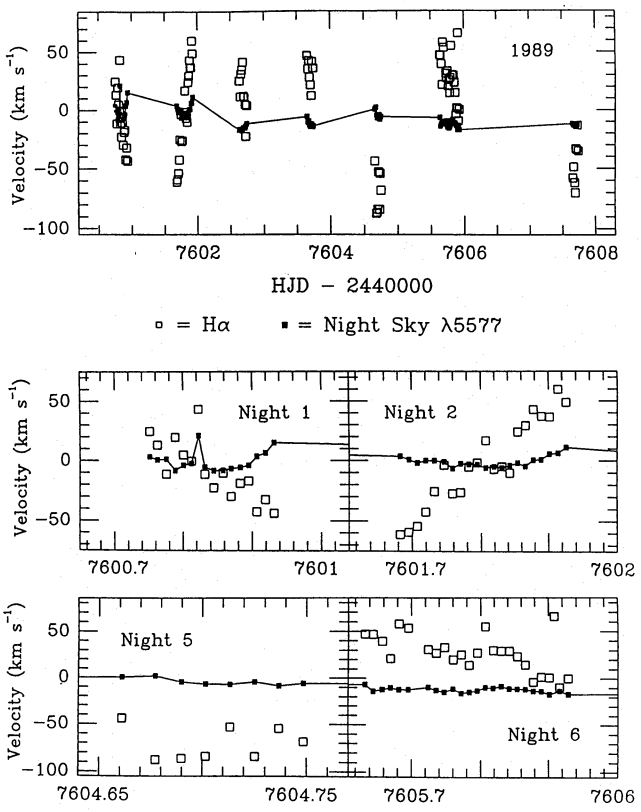

Figure 17. (Top) The reality of the quasi-periodic variations is supported by subtracting the orbit from the radial velocity curve and plotting the residual velocities (as open squares), which vary throughout each of the nights and not just from night to night. We also plot (connected filled squares) velocities of the O I λ5577-Å night-sky line. As they should be zero, they show the quality of the measured velocities: the deviations of the night-sky lines are of order ±10 km s^{-1}, typical for a Cassegrain spectrograph. Those of the Hα line easily exceed ±40 km s^{-1}. (Middle and Bottom) The residual velocities also vary continuously, as plots of the individual nights' velocities show.

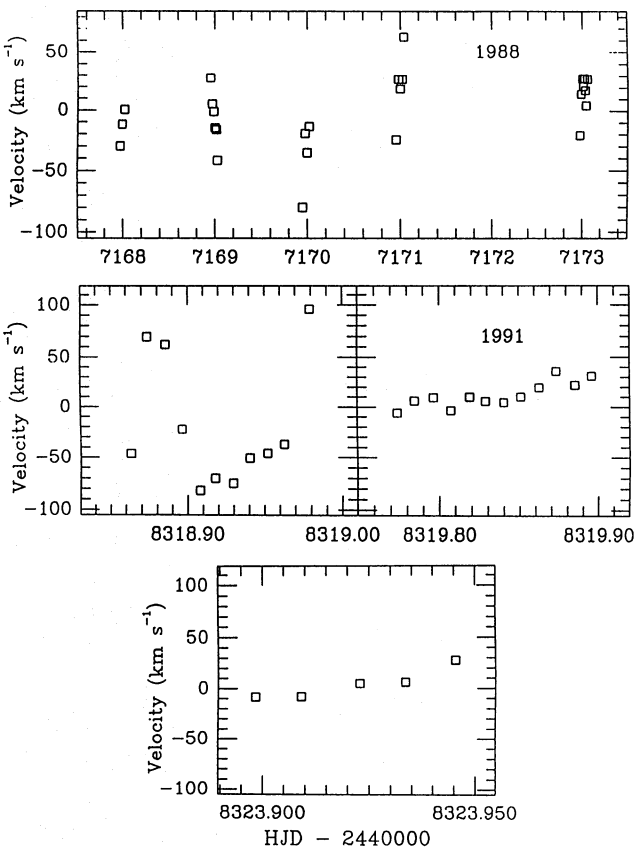

Figure 18. Similar diagram to Fig. 17, except plotting the 1988 and 1991 velocities. Unfortunately, the wavelength coverage did not permit night-sky measurements, but still the Hα velocities appear to wander in all three epochs.

tion discs: Patterson & Richman (1991) evoked them as an explanation for incommensurabilities between orbital and photometric periods, and Honey et al. (1988) detected a variable γ_{em} from a CV disc, thought to be due to disc waves associated with superhumps (Whitehurst 1988).

Other types of accretion disc waves may warrant consideration, too. We would not see quasi-periodic behaviour at any epoch unless such waves had a non-zero pattern speed. We tried binning the 1988 spectra on both the periodicities, to check for a V/R variation from an $m=1$ one-armed spiral wave (e.g. Spruit et al. 1987; Kato 1989). Results were inconclusive, since the S-wave muddied the line profile. Interestingly, though, a low-frequency V/R variation was present in V795 Her (Thorstensen 1986; see his fig. 14).

We caution that no proper statistical analysis for unevenly sampled, multiply periodic (or quasi-periodic) data is in common use in astronomy. The closest is that of Horne & Baliunas (1986), which treats two periodicities plus noise. A problem with the Lomb–Scargle periodogram is that it assumes the signal to be sinusoidal and the noise to be Gaussian-distributed. If two or more periodicities exist, these assumptions no longer hold and the noise can no longer be considered to be uncorrelated. Our approach of subtracting one periodicity at a time and then measuring the parameters of what is left, sometimes called 'prewhitening', leaves us with reservations about its statistical validity – it alters the data. It may well force γ_{em} for the anomalous velocity variations to zero, although we have by trial and error subtracted the periodicities in all orders possible and find no significant changes in the parameters in Table 1(c). It would be desirable to have a rigorous technique, however, particularly for error estimation in the presence of noise. Beats of any small modulation of the radial velocity curve may give the velocities their observed low-frequency quasi-periodicities, and noise variations in the velocities may well cause an apparent variability in period.

6 CONCLUSIONS

CZ Orionis is inferred to have an orbital period of 5.25 h. This is within 3 per cent of a prediction by Szkody & Mattei (1984), based on the empirical relation between outburst decline duration and orbital period (Bailey 1975). CZ Ori is an ordinary dwarf nova, similar to U Gem. After an outburst, the Hα radial velocity semi-amplitude, K_{em}, decreased slightly. A situation is demonstrated in which the periodogram for unevenly spaced data of Lomb (1976) and Scargle

(1982) is not equivalent to a least-squares spectrum, when the mean of the data is not the mean of the fit. We detect an M2.5 ± 1.0 secondary, and infer an absolute magnitude for this CV in R_{KC} of 8.5 ± 1.0 and estimate a distance of 260 ± 110 pc.

V1193 Orionis, also called Hamuy's Blue Variable, has an orbital period of 3.96 h. In 1988, the Hα line profile changed throughout the orbit, perhaps due to illumination of the red star. In 1989, the line profile had a peculiar variation, with the red wing of Hα flaring at phases 0.2 and 0.8. We estimate an absolute magnitude in R_{KC} of <5.9 and a distance of >470 pc, noting these are probably extreme limits, since they are based on not detecting the red star. V1193 Ori resembles UX UMa and IX Vel photometrically and spectroscopically, although it flickers fiercely. We also find yet another indication that CV emission lines do not reliably trace the motion of the white dwarf: the K velocity measured from Hα changed significantly between epochs, in this supposedly steady nova-like star.

BZ Ursae Majoris displays a 97.8-min spectroscopic period which we interpret as the orbital period. There is also significant low-frequency variation in velocities measured from the Hα line. While it is impossible to rule out completely an instrumental origin for this, we consider that the accretion disc may oscillate, or perhaps there is column accretion on to a magnetic white dwarf. Either case would be interesting: the first may be useful as a probe of disc physics, the second would indicate a new type of magnetic CV. Even if this is only an instrumental effect, though, it is important to understand its origin. A troubling thought arises: how many other times have these velocity variations been measured and interpreted as orbital periods? We therefore advise caution in interpreting the radial velocity curves of apparent long-period CVs, such as V795 Her. If some long-period CVs have their radial velocity curves remeasured, will they change? No explanation is satisfactory in present form, so we stress the need to confirm this finding with other instruments. A fibre-fed spectrograph with a circular aperture, for example, should reduce atmospheric dispersion and flexure effects.

We also deconvolve an M5.5 ± 0.5 red star from spectra of BZ UMa, find an absolute magnitude for this CV in R_{KC} of 10.7 (+0.7/−0.9) and estimate a distance of 110 (+44/−51) pc. A *JHK* photometric parallax gives a distance of >140 pc, so BZ UMa is a good candidate for a trigonometric parallax measurement.

ACKNOWLEDGMENTS

Observations were made at Michigan–Dartmouth–MIT Observatory (formerly McGraw–Hill Observatory), Kitt Peak, Arizona, which is owned and operated by a consortium of the University of Michigan, Dartmouth College and the Massachusetts Institute of Technology. Section 2 of this paper is based on a chapter in FAR's PhD thesis, Department of Physics and Astronomy, Dartmouth College. FAR and RMH were recipients of Dartmouth Fellowships during the observations and much of the preparation of this work, and FAR now holds a SERC/PPARC Postdoctoral Research Fellowship. We thank Bob Barr, Larry Breuer, Matt Johns and Peter Mack for their expert observatory support, and are grateful for discussions with Mario Hamuy, Joe Patterson, Ron Remillard, Allen Shafter, Paula Szkody and Richard Wade. (Curiously, Hamuy and Hamwey are Spanish and English spellings of the same Arabic name.) The AAVSO Director, Dr Janet A. Mattei, sent data from the international AAVSO data base and we thank all the observers who contributed. Special thanks are due to Janusz Kaluzny and to Paula Szkody, for respectively sending us their blue and infrared time-resolved photometry of BZ UMa. Our thanks also to Koji Mukai and Tim Naylor, who wrote the ARK software, with which some of the analysis was done, and adapted it to run on the Keele Starlink node.

REFERENCES

Bailey J., 1975, J. Br. Astron. Assoc., 86, 30
Bailey J., 1981, MNRAS, 197, 31
Berriman G., Szkody P., Capps R. W., 1985, MNRAS, 217, 327
Bessell M. S., 1986, PASP, 98, 1303
Bessell M. S., 1991, AJ, 101, 662
Beuermann K., Thomas H. C., 1990, A&A, 230, 326
Bond H. E., Grauer A. D., Burstein D., Marzke R. O., 1987, PASP, 99, 1097
Bruch A., 1989, A&AS, 78, 145
Bruch A., Fischer F.-J., Wilmsen U., 1987, A&AS, 70, 481
Cash W., 1979, ApJ, 228, 939
Claudi R., Bianchini A., Munari U., 1990, IAU Circ. No. 4975
Crosa L., Szkody P., Stokes G., Swank J., Wallerstein G., 1981, ApJ, 247, 984
Davey S., Smith R. C., 1992, MNRAS, 257, 476
Eggleton P. P., 1983, ApJ, 268, 368
Filippenko A. V., Ebneter K., 1986, IAU Circ. No. 4190
Friend M. T., Martin J. S., Smith R. C., Jones D. H. P., 1988, MNRAS, 233, 451
Green R. F., Ferguson D. H., Liebert J., Schmidt M., 1982, PASP, 94, 560
Green R. F., Schmidt M., Liebert J., 1986, ApJS, 61, 305
Hameury J. M., King A. R., Lasota J. P., 1991, A&A, 248, 525
Hamuy M., Maza J., 1986, Inf. Bull. Variable Stars, No. 2867
Hessman F. V., 1989, AJ, 98, 675
Hoffmeister C., 1928, Mitt. Sternw. Sonneberg 15
Honey W. B., Charles P. A., Whitehurst R., Barrett P. E., Smale A. P., 1988, MNRAS, 231, 1
Honeycutt R. K., Kaitchuck R. H., Schlegel E. M., 1987, ApJS, 65, 451
Horne J. H., Baliunas S. L., 1986, ApJ, 302, 757
Hurst G. M., Lubbock S., 1988, IAU Circ. No. 4691
Kaluzny J., 1986, IAU Circ. No. 4287
Kato S., 1989, in Meyer F., Duschl W. J., Frank J., Meyer-Hofmeister E., eds, NATO ASI Series C 290, Theory of Accretion Disks. Kluwer, Dordrecht, p. 173
Kirkpatrick J. D., Henry T. J., McCarthy D. W., Jr, 1991, ApJS, 77, 417
La Dous C., 1993, in Hack M., la Dous C., eds, Cataclysmic Variables and Related Objects. NASA/CNRS Monograph Series on Non-Thermal Phenomena in Stellar Atmospheres, NASA
Liebert J., Stockman H. S., 1980, PASP, 92, 657
Livio M., 1993, in Wheeler J. C., ed., Accretion Disks in Compact Stellar Systems. World Scientific, Philadelphia
Livio M., 1994, in Shore S., Livio M., van den Heuvel E. P. J., eds, Proc. 22nd 'SAAS FEE' Advanced Course, Interacting Binaries. Springer-Verlag, Berlin
Lomb N. R., 1976, Ap&SS, 39, 447
Luppino G. A., 1989, PASP, 101, 931
Markarian B. E., 1968, Afz, 4, 144
Mason K. O., Córdova F. A., Watson M. G., King A. R., 1988, MNRAS, 232, 779

Mattei J. A., 1992, IAU Circ. No. 5644
Mattei J. A., 1993, AAVSO Alert Notice 171
Maza J., Hamuy M., 1986, IAU Circ. No. 4172
Mukai K., Charles P. A., 1986, MNRAS, 222, 1P
O'Donoghue D., Chen A., Marang F., Mittaz J. P. D., Winkler H., Warner B., 1991, MNRAS, 250, 363
Oke J. B., 1974, ApJS, 27, 21
Oke J. B., Wade R. A., 1982, AJ, 87, 670
Patterson J., 1984, ApJS, 54, 443
Patterson J., Richman H., 1991, PASP, 103, 735
Plavec M., Kratochvil P., 1964, Bull. Astron. Inst. Czech., 15, 165
Press W. H., Teukolsky S. A., Vetterling W. T., Flannery B., 1992, Numerical Recipes in C, Second Edition. Cambridge Univ. Press, Cambridge, p. 575
Ramseyer T. F., 1994, ApJ, 425, 243
Ratering C., Bruch A., Diaz M., 1993, A&A, 268, 694
Ritter H., Kolb U., 1994, in Lewin W. H. G., van Paradijs J., van den Heuvel E. P. J., eds, X-ray Binaries. Cambridge Univ. Press, Cambridge
Robinson E. L., Zhang E.-H., Stover R. J., 1986, ApJ, 305, 732
Scargle J. D., 1982, ApJ, 263, 835
Schmeer P., 1990, IAU Circ. No. 5051
Schneider D. P., Young P. J., 1980, ApJ, 238, 946
Shafter A. W., 1983, ApJ, 267, 222
Shafter A. W., Harkness R. P., 1986, AJ, 92, 658
Shafter A. W., Wheeler J. C., Cannizzo J. K., 1986, ApJ, 305, 261
Shafter A. W., Robinson E. L., Crampton D., Warner B., Prestage R. M., 1990, ApJ, 354, 708
Silber A. D., 1992, PhD thesis, MIT
Smak J., 1984, PASP, 96, 5
Spogli C., Claudi R. U., 1994, A&A, 281, 808
Spruit H. C., Matsuda T., Inoue M., Sawada K., 1987, MNRAS, 229, 517
Stockman H. S., Schmidt G. D., Berriman G., Liebert J., Moore R. L., Wickramasinghe D. T., 1992, ApJ, 401, 628
Szkody P., 1985, AJ, 90, 1837
Szkody, P., 1987, ApJS, 63, 685
Szkody P., Feinswog L., 1988, ApJ, 334, 422
Szkody P., Mattei J. A., 1984, PASP, 96, 988
Thorstensen J. R., 1986, AJ, 91, 940
Thorstensen J. R., Freed I. W., 1985, AJ, 90, 2082
Thorstensen J. R., Ringwald F. A., Wade R. A., Schmidt G. D., Norsworthy J. E., 1991, AJ, 102, 272
Wade R. A. Horne K., 1988, ApJ, 324, 411
Warner B., 1976, in Eggleton P., Mitton S., Whelan J., eds, Proc. IAU Symp. 73, The Structure and Evolution of Close Binaries. Reidel, Dordrecht, p. 85
Warner B., 1987, MNRAS, 227, 23
Warner B., Nather R. E., 1988, Inf. Bull. Variable Stars, No. 3140
Wenzel W., 1982, Inf. Bull. Variable Stars, No. 2256
White N. E., Holt S. S., 1982, ApJ, 257, 318
Whitehurst R., 1988, MNRAS, 232, 35
Williams G. A., 1983, ApJS, 53, 523
Williams G. A., Hiltner W. A., 1984, MNRAS, 211, 629
Wood J. H., Hessman F., Fiedler A., 1990, in Mauche C. W., ed., Accretion-Powered Compact Binaries. Cambridge Univ. Press, Cambridge, p. 93
Wood K. S. et al., 1984, ApJS, 56, 507
Zhang E., Robinson E. L., Ramseyer T. F., Shetrone M. D., Stiening R. F., 1991, ApJ, 381, 534